Summer 6-2014

Sedimentological and Stratigraphic Study of a Falling-Stage Delta Complex in the Upper Cretaceous (Turonian) Ferron Sandstone Member of the Mancos Shale, South-Central Utah, USA

Fares Alaboud
University of Nebraska-Lincoln, f_m56@hotmail.com

SEDIMENTOLOGICAL AND STRATIGRAPHIC STUDY OF A FALLING-STAGE DELTA COMPLEX IN THE UPPER CRETACEOUS (TURONIAN) FERRON SANDSTONE MEMBER OF THE MANCOS SHALE, SOUTH-CENTRAL UTAH, USA

by

Fares Alaboud

A THESIS

Presented to the Faculty of

The Graduate College at the University of Nebraska

In Partial Fulfillment of Requirements

For the Degree of Master of Science

Major: Earth and Atmospheric Sciences

Under the Supervision of Professor Christopher R. Fielding

Lincoln, Nebraska

June, 2014

SEDIMENTOLOGICAL AND STRATIGRAPHIC STUDY OF A FALLING-STAGE DELTA COMPLEX IN THE UPPER CRETACEOUS (TURONIAN) FERRON SANDSTONE MEMBER OF THE MANCOS SHALE, SOUTH-CENTRAL UTAH, USA

Fares Alaboud, M.S.

University of Nebraska, 2014

Adviser: Christopher R. Fielding

The character and distribution of lithofacies in falling-stage deltas are incompletely documented. This paper presents a sedimentological and stratigraphic evaluation of a superbly-exposed interval of Cretaceous deltaic strata that are believed to be of falling stage origin. The studied interval forms part of the Upper Cretaceous (Turonian) Ferron Sandstone Member of the Mancos Shale in the southernmost Henry Mountains Basin of south-central Utah, USA. The interval of interest is exposed in three dimensions over a 20 km^2 area in a series of canyon walls. Observed facies include fine-grained mudrocks (offshore basin), mudrocks with thinly interlaminated sandstone (prodelta), thinly interbedded siltstones and fine-grained sandstones (distal delta front), thickly interbedded siltstones, coarse-grained siltstones and fine-grained sandstones (medial delta front), and amalgamated fine- to medium-grained sandstones (proximal delta front). No facies of interpreted delta top origin were observed within the studied succession. The proximal delta front facies includes spectacular, chaotic sandstone-filled gullies up to 6 m deep and 300 m wide. The basal parts of these gully fills preserve large-scale convolute bedding, rotational failures and, in numerous places, growth faults. At

least three such gully fills were noted, incised into different levels within the succession. The existence of three gully fills indicates episodes of delta progradation and sea level fall. Paleocurrent data indicate southeastward sediment dispersal. Facies stacking patterns and incised gully fills, together with the lack of a delta plain topset, argue strongly for a falling stage origin for the described succession. This study provides new insights into the facies architecture and stacking patterns of shallow-water, falling-stage deltas. In particular, the study illustrates a style of falling-stage deltaic system in which a descending regressive trajectory is difficult to discern.

Acknowledgments

The completion of this thesis would not have been possible if not for certain individuals that I would like to recognize. First, I express my sincere gratitude to my parents overseas for their unlimited encouragement and support. I would like to dedicate special thanks to my wife Rasha Alzaidan, who was my biggest supporter during my studies and research, for her support, patience, and encouragement. Also I thank my daughter Laura for her smiles, love, and patience. I would like to thank my brothers and sisters for their encouragement and support.

I would like to express my full gratitude and sincere thanks to my advisor Dr. Christopher Fielding for his immense assistance and advice during the completion of this project. I appreciate his wisdom, support, consistent professional guidance, and continuous encouragement. The success of this research would have not been possible if not for his guidance and support. I would like to extend my gratitude to Dr. Tracy Frank and Dr. David Loope for being a part of my committee. I would also like to thank the University of Nebraska-Lincoln Department of Earth and Atmospheric Sciences for offering me the opportunity to conduct graduate level research.

This research was made possible through funding provided by Saudi Arabian Oil Company (Saudi Aramco). I would like to thank Saudi Aramco for sponsoring my master's studies and providing funds for my fieldwork.

Table of Contents

INTRODUCTION

Cretaceous deposits of the Western Interior Seaway (WIS) basin of North America, many of which are of deltaic origin, are spectacularly exposed in terms of quality and lateral extent as cliff sections in the modern southwest of the USA. These deltaic deposits consist of sandstone bodies encased in marine mudstones, and are believed to be sourced from the Sevier Orogenic Highlands to the west of the Cretaceous Western Interior Seaway (KWIS). The lower Upper Cretaceous (Turonian) Ferron Sandstone Member of the Mancos Shale is one of these deltaic units. Three delta complexes issuing eastward into the Cretaceous Western Interior Seaway formed the Ferron Sandstone. These deltas complexes are, from north to south, the Vernal, Last Chance, and Notom Deltas (Cotter 1975; Hill, 1982) (Fig. 1).

The Ferron Sandstone was originally described by Lupton (1916) in the type area near the town of Ferron, Utah, which is to the north of the Henry Mountains. The Notom Delta is well exposed in the Henry Mountains region, and the Ferron Sandstone outcrops along the western side of the mountains with continuous cliff vertical exposures along north-south and canyons that cut east-west. The Ferron Sandstone shows a general coarsening upward from offshore mudstones to coarse-grained sandstone deposits and is interpreted to be a result of delta complexes building out into a shallow sea (Hill, 1982; Bhattacharya & Davis, 2004; Fielding, 2010; Li et al., 2011b).

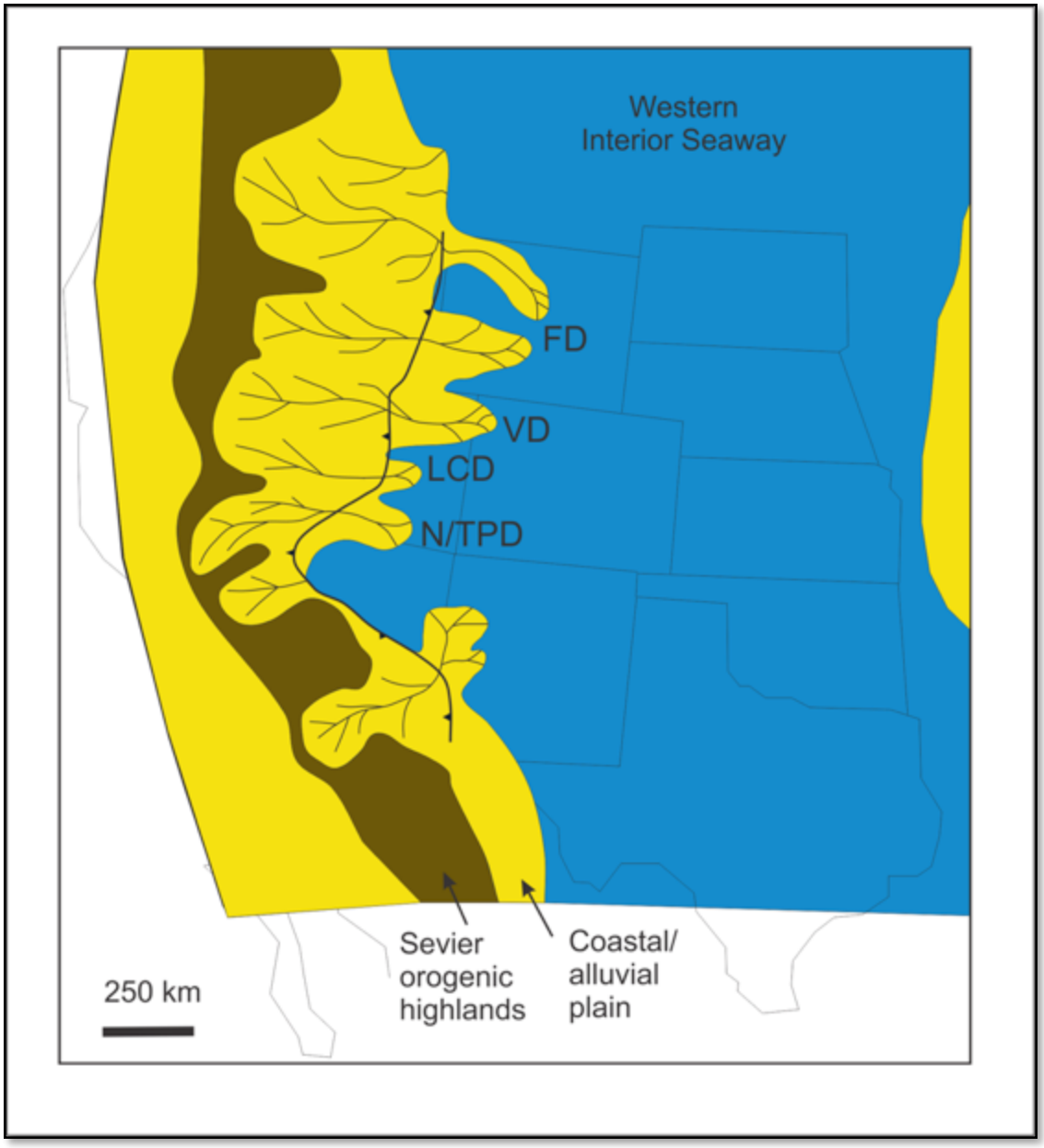

Figure 1: Paleogeographic reconstruction of the Cretaceous Western Interior Seway (KWIS) of North America during Upper Cretaceous (Turonian) time. Several delta complexes issued into KWIS as shown, several deltas issued into the KWIS. These deltas are Frontier Delta (FD), Vernal Delta (VD), Last Chance Delta (LCD), and Notom Delta (N/TPD) (Fielding, 2011).

The Ferron Sandstone has been divided into two informal, upper and lower members (Peterson and Ryder, 1975). This study is concerned with a delta lobe within the lower member of the Ferron Sandstone. A series of coarsening upward cycles within

the lower member consisting of delta-front sandstones separated by thin recessive mudstone suggest a long-term regime of decreasing accommodation with superimposed, higher-frequency fluctuations giving rise to individual cycles (Fielding, 2010). Relative sea-level fluctuations are believed to have been generated from allogenic controls (climate, tectonic, eustacy) (Fielding, 2010; Zhu et al., 2012). The lower member contains sandstone bodies that are believed to have been formed under forcing by relative sea-level fall (Fielding, 2011). The preservation potential of the falling-stage strata is in general low (Posamentier & Morris, 2002; Plint & Nummedal, 2002; Catuneanu, 2006). In this paper, I show evidence of falling-stage deposition within one component delta lobe within the lower Ferron Sandstone.

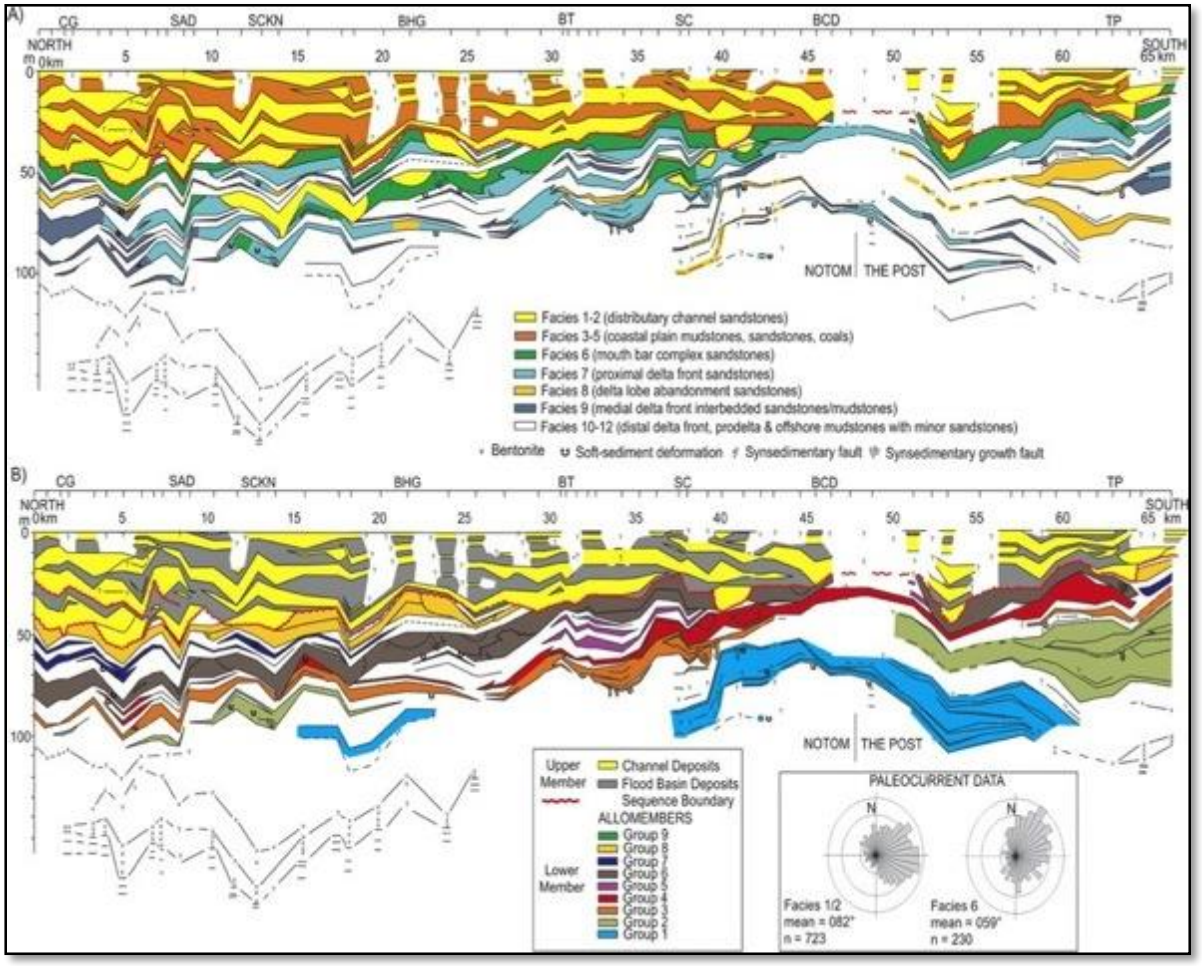

Figure 2: Detailed cross sections oriented in a north-south (depositional strike) direction through the Ferron Sandstone Member of the Mancos Shale along the western flank of the Henry Mountains syncline in south-central Utah, USA. A: Cross section color coded by lithofacies (after Fielding, 2010). B: cross section color coded by genetically related bedsets (allomembers) separated by surface of apparent hiatus. The two sections are hung from top of Ferron Sandstone (Fielding, 2011).

OBJECTIVES:

The purpose of this study is to evaluate the origin of one component deltaic unit within the Cretaceous Ferron Sandstone Member, which is exposed around the limbs of the Henry Mountains in south-central Utah, using facies analysis and stratal stacking

patterns based on field observations. The Henry Mountains Cretaceous strata have not been as intensively studied as other outcrops such as Book Cliffs to the northeast, Wasatch Plateau to the north, and Kaiparowits Plateau to the southwest (Fielding, 2010; Li et al, 2011,2012). My study of a deltaic unit within the Ferron Sandstone will add to the understanding of the Cretaceous deltas in the Western Interior Seaway (KWIS) of North America. The outcome of this study will improve the understanding of the regional sequence stratigraphy of the whole formation and will aid in understanding similar units within KWIS. The Ferron Sandstone Member of the Mancos Shale Formation contains important coal beds and is a target for both conventional and unconventional petroleum exploration. This study will provide important information relevant to future development of hydrocarbon exploration in the region.

GEOLOGIC BACKGROUND:

The Ferron Member of the Mancos Shale Formation was deposited during the Turonian stage of the Cretaceous along the western margin of the Cretaceous Western Interior Seaway (KWIS). The Ferron and equivalent parts of the Frontier Formation in northern Utah and Wyoming record widespread regression of the KWIS (Fig. 3). The Ferron Member was formed as series of clastic wedges that were shed from the Sevier orogenic belt to the west into a foreland basin to the east (Hale 1972; Cotter 1975; Ryer & Anderson, 2004) (Figs. 1, 3).

During late Early Cretaceous time, rapid subsidence of a foredeep immediately east of the Sevier orogenic belt took place. This subsidence continued through early Late Cretaceous time. In the Cenomanian, the foredeep was strongly elongate and extended

throughout Utah. Later on, during Turonian through Santonian time, subsidence became concentrated in northern Utah and southwestern Wyoming and decreased in southern Utah. Shoreline encroachment reached tens of kilometers towards the Sevier orogenic belt in some areas and the sea submerged the region. The Tununk Shale was accumulated in central Utah at this time. During middle Turonian time, the shoreline prograded towards the east with regression of the KWIS (Ryer & Anderson, 2004). This regression is marked by the deposition of the Ferron Sandstone in central Utah and the Frontier Formation in northern Utah (Fig. 1). The subsidence was rapid in northern Utah, but sediment supply was high enough to fill the depositional space to compensate for subsidence. Subsidence in central and southern Utah, however, was less; and subsidence and sediment supply were more evenly balanced. Rapid transgression occurred during Coniacian time, where the sea transgressed across the Ferron coastal plain to a position near the western edge of the Wasatch Plateau (Ryer & Anderson, 2004). The lack of Coniacian deposits in the Henry Mountains basin suggests that an unconformity exists between the Ferron and overlying marine shales of the Blue Gate Shale in the region (Zhu et al., 2012).

Figure 3: North America during the Upper Cretaceous (Turonian), with the Cretaceous Western Interior Seaway (KWIS) dividing the continent (Ron Blakey, NAU Geology).

This study concerns deposits of the Notom Delta in south-central Utah (Fig. 1). The unit is exposed along the northern and western sides of the Henry Mountains in south-central Utah (Fig. 4). The surface exposure in the Henry Mountains is excellent in terms of quality and lateral extent, which makes it a great place for geological studies. The Henry Mountains Syncline is a structural basin that is one of the major folds of the Colorado Plateau. The Henry Mountains themselves are composed of five individual mountains that are separated by low passes and each is a structural dome that is produced

by laccoliths. These domes are related to deformation by physical injection of the stocks. The syncline lies between the Waterpocket Fold to the west and the Monument upwarp to the east of the syncline (Fig. 5). The syncline is north-south elongate extending around 80 kilometers along the axis (Hunt, 1946; Hunt et al., 1953; Bon, 2005). Gilbert (1877) was the first to investigate the Henry mountains area. He named the Ferron unit the Tununk Sandstone and the underlying marine shale the Tununk Shale. The name Tununk Sandstone was discarded and replaced with the name Ferron Sandstone Member by Hunt and Miller (1946) after correlating the unit with the type Ferron section originally described by Lupton (1916) near the town of Ferron, Utah. Hunt and others (1953) were the first to recognize the erosion surface between the Ferron and the Blue Gate Members and divided the Ferron Sandstone into three units. Peterson and Ryder (1975) studied the Cretaceous rocks in the Henry Mountains region including the Ferron Sandstone Member. They changed the three-units division by Hunt and others of the Ferron into two units differing in lithologic characteristics and depositional environments, which help in distinguishing them. The lower unit lies conformably above the Tununk Shale, and the upper unit is separated from the Blue Gate Shale by an unconformity. They measured 22 sections of the Ferron Member along the north, west, and south sides of the Henry Mountains and found that it ranges in thickness from 62 to 117 meters with the average being 93 meters. More work on the Ferron Sandstone was carried out by Uresk (1979), Hill (1982), Smith (1983), Morton (1984), Whitlock (1984), Eaton (1990), Fielding (2010, 2011), Li and others (2010, 2011, 2012), and Zhu et al. (2012).

The Ferron Sandstone Member of the Mancos Shale is interpreted as the deposits of fluvial and wave-influenced deltas that issued eastward into the Western Interior Seaway basin (Fielding, 2010, Li et al., 2011). The Turonian Ferron is bounded by the Blue Gate Shale Member above and the Tununk Shale Member below (Fig. 6). The deltaic Ferron sandstone can be divided into upper and lower members (Peterson and Ryder, 1975). The two members are separated by an abrupt erosional boundary that can be traced for long distance and is interpreted to be a major sequence boundary (Fielding, 2011). The lower member is made up of generally coarsening upward progradational cycles, while the upper member consists of erosionally-based, nonmarine sandstone bodies that are interbedded with mudstone, coal, and carbonaceous shale (Hunt et al., 1953; Peterson & Ryder 1975; Hill, 1982; Fielding, 2010). Deltaic sandstone bodies at the base of the lower member are, generally, thin and relatively laterally restricted. They become thicker, more laterally amalgamated, and broader in the depositional strike orientation upward (Fig. 2).

Hill (1982) interpreted the Notom delta as a birdsfoot, fluvially-dominated delta with minor reworking of sediments by wave action. He proposed a modern analog of Guadalupe River Delta of the Texas Gulf Coast for Ferron sandstone deposition rather than the Mississippi River Delta as proposed by Cotter (1975). Fielding (2010) proposed the Holocene Burdekin River Delta of NE Australia as a modern analog for the Ferron Notom delta. Fielding (2011) mapped the Ferron Sandstone exposure over 67 km in a strike section (Fig. 2) and was able to track the abrupt erosional boundary separating the two members over that distance and interpreted it as a sequence boundary. Li and others (2010, 2011, 2013) studied the Ferron Notom delta to evaluate delta asymmetry using

sedimentological and ichnological observations. They recognized six sequences within the Notom deltaic complex.

Twelve lithofacies were identified in the Ferron sandstone by Fielding (2010). The facies can be grouped into two main associations that represent the upper and the lower members. Facies representing the upper member comprise delta plain deposits, while the facies of the lower member consist of marine deposits of the delta and open marine deposits beyond the delta. Zhu and others (2012) combined available ammonite biostratigraphy of the Ferron Notom Delta Complex with absolute ages obtained from $^{40}Ar/^{39}Ar$ dating of sanidine crystals in the Ferron bentonites to establish the chronology of the delta (Table 1). The lowest and oldest bentonite bed was found to have an age of 91.25 +/- 0.77 Ma, which indicates that the Ferron Notom Delta Complex was initiated around 91.25 Ma. The uppermost bentonite in the Ferron Member (near the top of the upper member) has a calculated age of 90.64 +/- 0.25 Ma. The bentonite bed that lies immediately above the Ferron–Blue Gate contact has a calculated age of 87.27 +/- 0.54 Ma. The large jump in age from the last two bentonite beds supports the notion that an unconformity lies between the Ferron Sandstone and the Blue Gate Shale. The top of the Ferron is estimated to have an age of 90.63 Ma; which means that the Ferron Notom Delta Complex was deposited between 91.25 Ma and 90.63 Ma for duration of 620,000 years (Zhu et al., 2012).

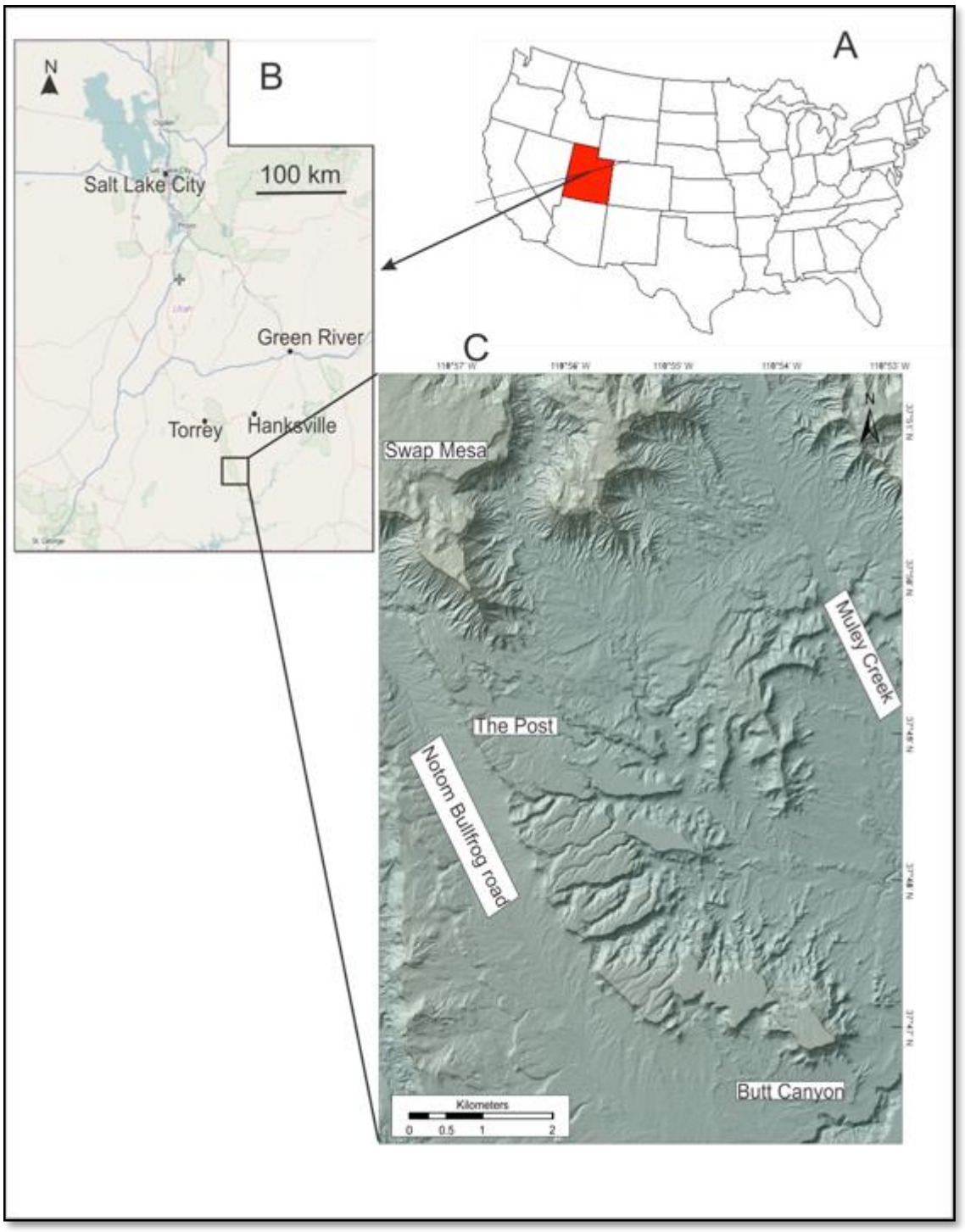

Figure 4: Location of the study area. A: Map of the United States with Utah State highlighted in red. B: Map of Utah with rectangle showing study area along western limb of Henry Mountains. C: Digital Elevation Model of the study area showing exposures of the Ferron Sandstone in study area between The Post, Muley Creek, and Butt Canyon. Series of canyons running SW-NE and other directions give rise to spectacular, three-dimensional exposures of the studied rocks.

Sample #	N	MSWD	Weighted Mean Age (Ma) ± 2s
UH-BHA-B5	8 of 8	0.27	87.27 ± 0.54
UH-BHA-B4	16 of 16	0.84	90.64 ± 0.25
UH-BHA-B3	12 of 14	1.05	90.69 ± 0.34
UH-BHA-B1	13 of 13	0.69	91.25 ± 0.77

Ages calculated relative to the 28.201 Ma Fish Canyon sanidine standard (Kuiper et al. 2008) using the decay constants of Min et al. (2000). Full data tables are available from the JSR Data Archive, see Acknowledgements section.

Table 1: Summary of $^{40}Ar/^{39}Ar$ dating of sanidine crystals from bentonite beds in the Ferron Notom Delta Complex (Zhu et al., 2012).

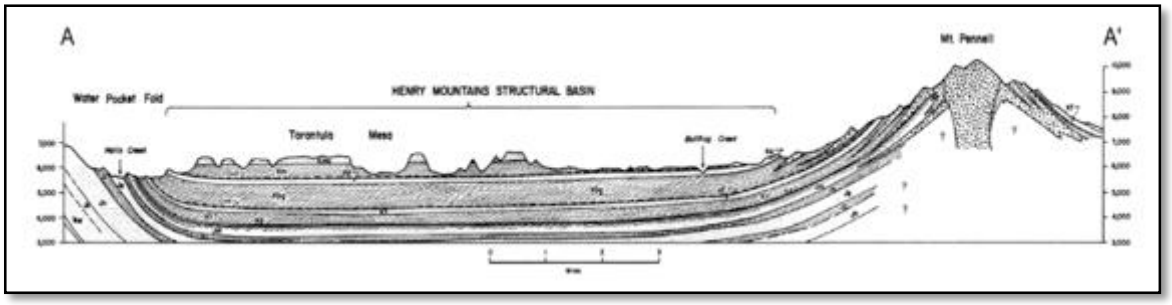

Figure 5: Idealized cross section of the Henry Mountains structural basin in a west-east direction (Bon, 2005).

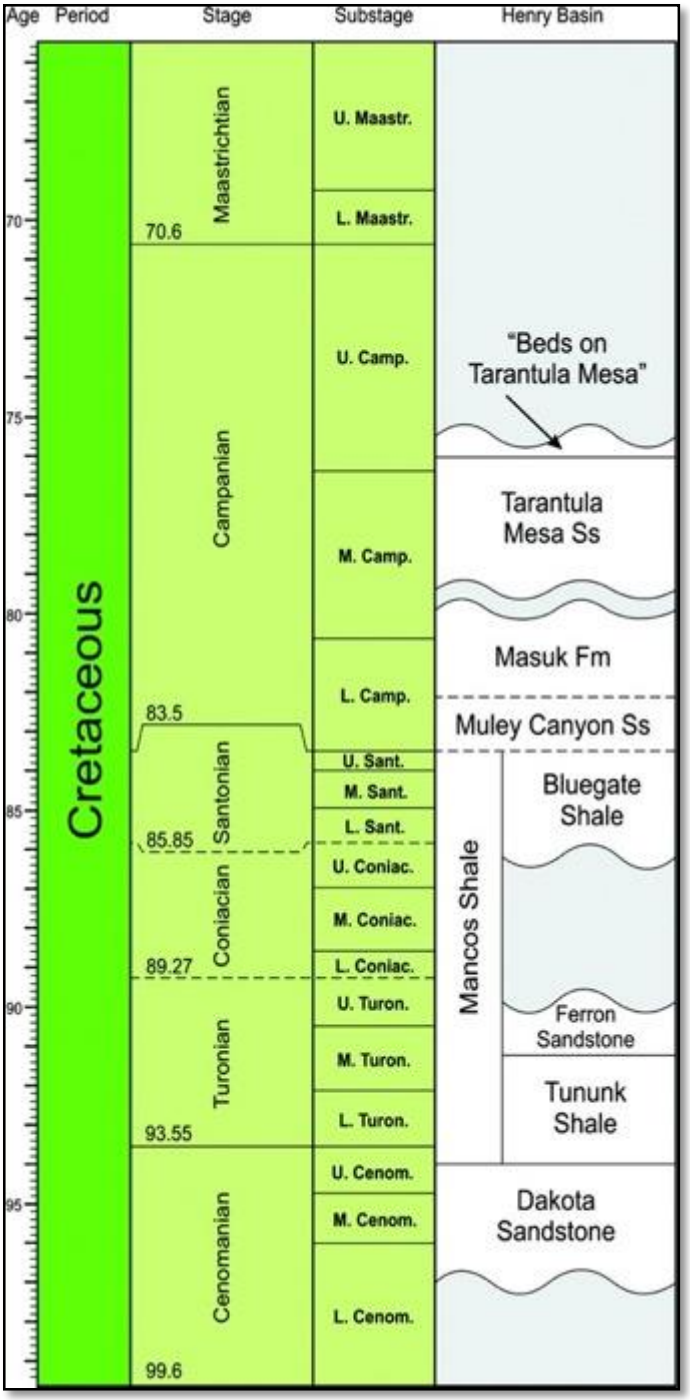

Figure 6: Stratigraphic column of the Upper Cretaceous successions in the Henry Mountains region (Fielding, 2010).

METHODS

An outcrop study of the Ferron Sandstone exposures in South-Central Utah was performed. A detailed sedimentological and ichnologic analysis were carried out over a 20 km^2 area. A total of fourteen detailed vertical sections were measured in the field. Collection of sedimentological and ichnologic data was performed, including lithology, grain size, sedimentary structures, beds contacts, vertical grain size trends, trace fossils, lateral variations, and paleocurrent data. These data were later used for depositional environment and stratigraphic analysis. Bioturbation index after Reineck (1963) was used, where bioturbation intensity is given a value from zero to six based on the degree of observed sediment distortion. Values of zero indicate the lack of bioturbation, while values of six represent complete sediment reworking by organisms (MacEachern and Bann, 2008). Examination of canyon walls led to the recognition of three gully fills at different horizons extending in a depositional dip direction. A series of canyons cutting the outcrop in a depositional strike direction (SW-NE) allowed for 3D view of the exposure and physical correlation to establish lateral continuity.

Measured sections were arranged in cross-sections along depositional strike (SW-NE) and depositional dip (NW-SE), which helped in correlating units and showing facies variations (Fig. 7). A basal bentonite bed, which lies within the shelfal marine shales of the upper Tununk Shale, was used as a datum for the cross-sections where available. This bentonite bed is laterally persistent and can be used as a stratigraphic marker. Where the basal bentonite was not exposed, a persistent tabular sandstone bed some 30-40 m higher in the section was used instead.

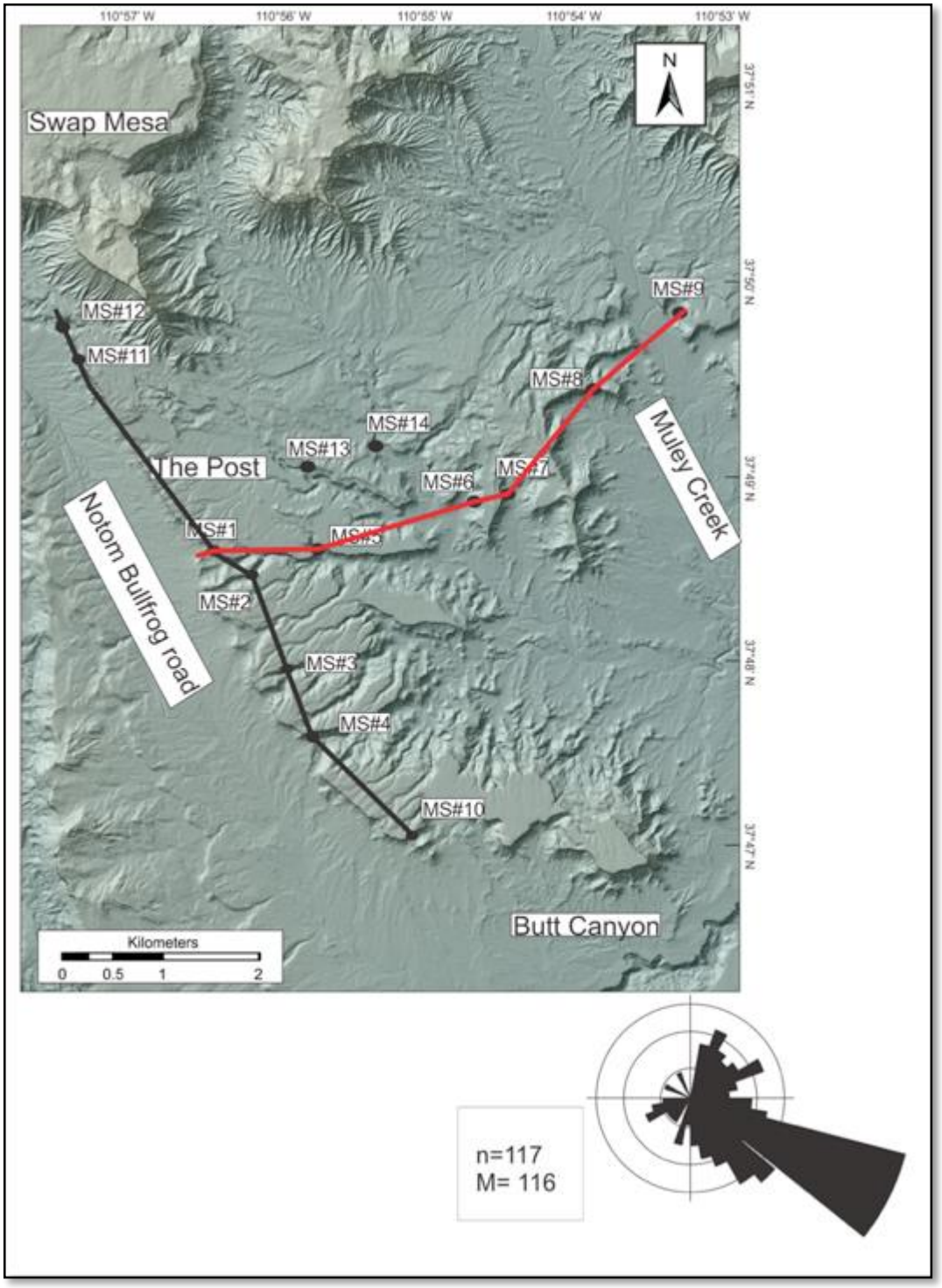

Figure 7: Map of the study area with cross-sections shown in colors. Black line shows cross-section in depositional dip direction; red line represents cross section in depositional strike section (see Figs. 17 & 18 for cross sections). Paleocurrent data indicate a mean southeast sediment dispersal. n: number of data collected; M: mean direction.

FACIES ANALYSIS

Five facies were observed within the studied units of the lower Ferron Sandstone Member of the Mancos Shale (Appendix 4: Facies Table). These facies include fine-grained mudrocks, mudrocks with thinly interlaminated sandstone, thinly interbedded siltstones and fine-grained sandstones, thickly interbedded siltstones, coarse-grained siltstones and fine-grained sandstones, and amalgamated fine- to medium-grained sandstones. The vertical sections show generally coarsening upward successions, starting from basal mudrocks through interbedded siltstone and sandstone to amalgamated sandstone at the top. The observed facies in the study area represent a subset of those described by Fielding (2010) within the Ferron Sandstone. The facies carry evidence for wave and fluvial influences on a broadly deltaic depositional environment. Following is a detailed analysis of these facies.

Facies 1

Description

Facies 1 is composed of black to dark grey, thinly laminated, fine-grained siltstones and claystones, with thin local bentonite beds (Fig. 8a). The claystones are fissile (shale) with fine laminations. The siltstone ratio increases up-section. The bentonite beds within these deposits are thin and are cream to light gray in color. Some bentonite beds are weathered deeply and exhibit a popcorn texture at surface. Facies 1 in the study area is largely unbioturbated with a bioturbation index (BI) of zero. The thickness of the intervals represented by these facies is tens of meters and reaches up to 45 m.

Interpretation

The dominance of mudrocks indicates deposition in offshore environments away from the reach of the delta. Hypopycnal plumes, resulting from differences in the densities of ambient and introduced waters, can carry sediment in suspension and transport it from a proximal source basinward (Bhattacharya, 2010; Plint, 2010). Clay and silt particles were deposited predominantly as sediment fall-out from suspension. As the plume density decreases, suspended sediments were deposited slowly forming continuous clay and silt accumulations. The lack of bioturbation in these facies suggests poorly oxic and reducing conditions (Bhattacharya & MacEachern, 2009). The increase in silt ratio up-section indicates deposition closer to the terrestrial source. Bentonite beds were deposited as a product of volcanic activity, where ash and lapilli were showered through the water column and accumulated on the sea floor (Fielding, 2010).

Facies 2

Description

Facies 2 consists mainly of laminated dark grey siltstone, with a minor constituent of thinly interbedded very fine- to fine-grained sandstone (Fig. 8B). Siltstones are finely laminated and fissile in places. Sandstone beds are thin and show ripple cross-lamination, planar to low-angle cross-bedding, and small hummocky cross-stratification (HCS). In places, small syneresis cracks were observed. The siltstones and sandstone contain local plant debris. The sandstone bodies have sharp upper and lower contacts. Thickness of sandstone beds varies, ranging from 0.07 – 0.15 m, where thicker beds are continuous

and thinner beds are restricted laterally. The sandstone ratio and thickness increase vertically up-section. Bioturbation in theses facies is rare and sporadic, mostly restricted to sandstone bed bases and tops. Facies 2 exhibits an overall bioturbation index (BI) of 0-3. Observed traces include *Planolites*, *Protovirgularia*, *Lockeia*, and small *Diplocraterion*. The trace fossils are diminutive in size and any one bioturbated bed typically has low trace diversity, with a maximum of three different ichnogenera.

Interpretation

Facies 2 was deposited in a more proximal environment than Facies 1. This is evident by the occurrence of sandstone beds and the increase of siltstone abundance in the expense of claystone. Fine mud and silt is interpreted to have settled slowly out of suspension in the absence of outflow. Distal portions of storm-flows are responsible for the deposition of the thin sandstone beds with unidirectional and combined-flow ripple cross-lamination. Low bioturbation intensity in these facies indicates a highly stressed environment. Salinity fluctuation is inferred by the sporadic and low bioturbation as well as syneresis cracks (Bhattacharya & MacEachern, 2009). The traces are diminutive and uncommon and the predominance of simple facies-crossing traces, *Diplocraterion* and *Planolites*, suggests the action of trophic generalists, where short-lived, opportunistic species exploit ecospace intermittently between storm events (MacEachern & Bann, 2008; Bhattacharya & MacEachern, 2009). The presence of sandstone beds, and the increase of siltstone abundance in the expense of claystone indicate a more proximal depositional environment than Facies 1. Therefore, Facies 2 is interpreted to represent deposition in a prodelta environment (Fielding, 2010).

Facies 3

Description

Facies 3 consists of thinly interbedded siltstone and sandstone (Fig. 8C). The siltstones are fine-grained to coarse-grained, and dark to medium gray in color. Coarse-grained siltstone beds are up to 0.2 m thick. The sandstones are very fine- to fine-grained. The thickness of sandstone bodies range from mainly 0.15 m to 0.2 m. Observed sedimentary structures in these facies include hummocky cross-stratification (HCS), Ripple cross-lamination, flat lamination, and low-angle cross-bedding. Some sandstone bed tops have wave ripples. Local plant debris can be observed in these facies, and are abundant in places. Some sandstone beds show soft sediment deformation (SSD). Sandstone bodies thicken and become more abundant up-section (Fig. 8D). The sandstone bodies here are more laterally continuous than Facies 2, and thicker in general. These sandstone bodies have sharp contacts with underlying siltstones. Low bioturbation intensity was observed in Facies 3, with bioturbation index (BI) of 0-2. The bioturbation is mainly restricted to sandstone beds. Observed trace fossils within these facies include *Planolites*, *Diplocraterion*, *Lockeia*, and *Cylindrichnus*. The trace fossils are diminutive in size and a bioturbated bed typically exhibits low trace diversity, with no more than two ichnogenera. In general, Facies 3 occurs repeatedly throughout the sections and it ranges in thickness from 1 – 12 m.

Interpretation

Sandstone bodies are thicker, more abundant, and laterally continuous than Facies 2, which indicates a more proximal depositional environment. Sedimentary structures observed within sandstone bodies indicate oscillatory, unidirectional, and combined flow deposition during storms in shallow marine settings (Hunter & Clifton, 1982; Southard et al., 1990; Arnott & Southard, 1990; Dumas et al., 2005). The sedimentary structures indicate that storm waves reworked Facies 3 as it was deposited (Bhattacharya & MacEachern, 2009). HCS is produced by combined flow with a strong oscillatory component (Dumas et al., 2005; Plint, 2010). HCS forms exclusively above storm wave base (Plint, 2010). Small subaqueous dunes that form small cross-bedding are related to strongly unidirectional flow (Dumas et al., 2005). Low bioturbation intensity (BI=0-2) in these facies indicates a highly stressed environment. The sporadic distribution of the bioturbation, diminutive sizes, and facies-crossing character of the trace-fossil represent a stressed expression of the *Cruziana* Ichnofacies (MacEachern & Bann, 2008; Bann et al., 2008). The low bioturbation could be related to rapid deposition during large storms (Bann et al., 2008; Bhattacharya & MacEachern, 2009). The range of traces indicates that bioturbation is likely the work of trophic generalists and opportunistic organisms inhabiting a highly stressed environment. Facies 3 is interpreted to be deposited in a distal delta front environment under the influence of waves, storms, and river outflow above storm wave base.

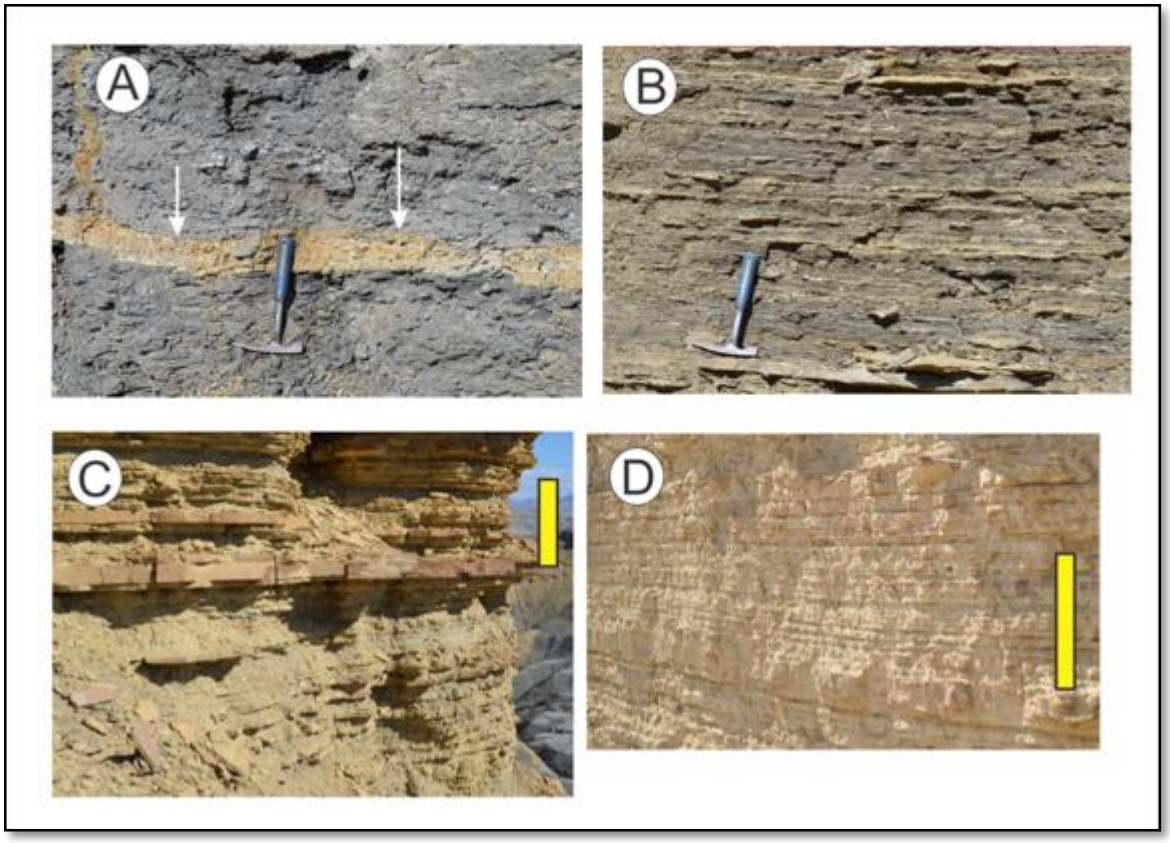

Figure 8: Photographs showing characteristics of Facies 1-3 observed throughout the study area. A) Black offshore shale (Facies 1) with thin bentonite bed (White arrows). Photo was taken near MS#5. B) View of prodelta facies (Facies 2). Dark gray siltstone interlaminated with sandstone. Photo was taken at MS#3, 1 m above base of described section. C) Thinly interbedded sandstone and siltstone of distal delta front (Facies 3). Photo was taken at MS#4, 62 m above base. Yellow bar is 1 m. D) Variant of Facies 3 towards the top of the section, showing increased sandstone ratio and thickness. Yellow bar is 1 m.
See Fig.7 for section locations & Appendix 2 for graphic logs. Hammer is 28 cm tall.

Facies 4

Description

Facies 4 contains thickly interbedded siltstone and sandstone (Fig. 9A). The siltstones are fine-grained to coarse-grained, and some coarse-grained siltstones show distinctive spheroidal weathering. Sandstone beds are very fine- to fine-grained and have

sharp contacts with underlying siltstones (Fig. 9B). The thicknesses of sandstone bodies range from 0.2m to 1.3m. Observed sedimentary structures within these individual sandstone beds include hummocky cross-stratification (HCS), ripple cross-lamination, flat-to-low angle cross-bedding, convolute bedding, soft-sediment deformation (SSD), wave ripples (on top of sandstone beds), and loading. SSD is common and pervasive in places (Fig. 9C). Some sandstone beds are massive. Some intervals contain shell and plant debris. In places, sandstone beds contain silt partings, syneresis cracks (Fig. 9D), sole marks, and gutter casts on bed bases. Some intervals show a general coarsening- and thickening-upward character. Siltstones lack bioturbation, while the sandstones show low to moderate bioturbation intensity (BI= 1-3). The bioturbation intensity differs from bed to bed, with some beds showing high bioturbation and others are largely unbioturbated. Observed ichnogenera include *Planolites, Lockeia, Teichichnus, Thalassinoides, Diplocraterion, Gyrochorte, Rhizocorallium, and Taenidium*. The trace fossils are mainly diminutive in size, and most of the beds have low diversity with one or two ichnogenera. Other beds, however, show higher diversity of trace fossils with up to four different ichnogenera. Facies 4 occurs throughout the study area towards the top of the sections, right below Facies 5. The overall thickness of these facies varies throughout measured sections, ranging from 2 – 12 m. Thicker, more laterally continuous sandstone beds in these facies when compared to Facies 3.

Interpretation

The abundance, thickness, and lateral extent of sandstone bodies within Facies 4 indicate a more proximal environment than Facies 3. The thicker sandstone bodies (up to

1.3m) indicate that sands were deposited during large river floods or major storms (Bhattacharya and Davis, 2004; Bhattacharya & MacEachern, 2009). Outflows were responsible for depositing discrete sandstone beds. The siltstones within this facies were deposited as sediment fallout from suspension, either passively or from turbulent plumes that were generated during storm outflows (Fielding, 2010). Sedimentary structures observed within sandstone bodies indicate oscillatory, unidirectional, and combined flow deposition during storms in shallow marine settings (Hunter & Clifton, 1982; Southard et al., 1990; Arnott & Southard, 1990; Dumas et al., 2005). Storm waves reworked the delta-front deposits, which resulted in these oscillation and combined-flow structures (Bhattacharya & MacEachern, 2009). Repeated hyperpycnal river floods and associated turbulent plumes resulted in deposition of interbedded unbioturbated mudstones and discrete beds of sand showing oscillation, wave, and current characters (Li et al., 2011). High sedimentation rates in the sandy beds are indicated by SSD (Bhattacharya & Davis, 2001; Porebski & Steel, 2005; MacEachern et al., 2005; Bhattacharya & MacEachern, 2009). Rapid deposition commonly resulted in soft-sediment deformation features (including loading and convolute bedding), and formation of fluid muds that generated soupground substrates (MacEachern et al., 2005). Low to moderate bioturbation (BI= 1-3) in sandstone beds indicates environmental stresses acted on these rocks during deposition. Observed ichnogenera indicate a proximal expression of the *Cruziana* Ichnofacies (MacEachern & Bann, 2008). The stressed trace fossil suite in most of the beds is likely to indicate a periodically brackish environment. This interpretation is also supported by the presence of syneresis cracks, which reflects clay shrinkage associated with salinity changes (MacEachern et al., 2005). Salinity reduction indicates proximity to

fluvial discharge. Therefore, Facies 4 is interpreted to be deposited in medial delta front environment, with river, wave and storm influence.

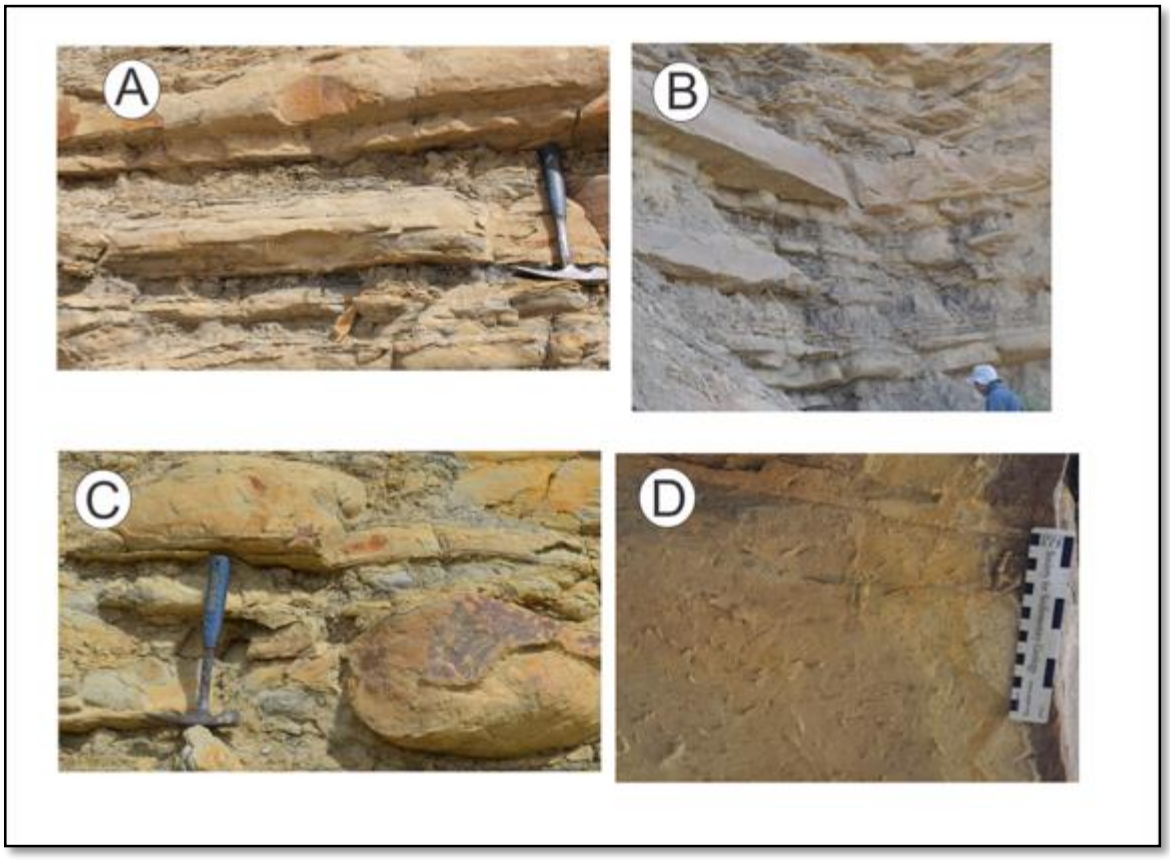

Figure 9: Photographs of Facies 4 (proximal delta front) throughout the study area. A) Thickly interbedded siltstone and sandstone. Photo was taken at MS#1, 45 m above base. B) Sharp-based sandstone bodies of Facies 4. Photo was taken at MS#11, 47 m above base. C) Soft-sediment deformation (SSD) within Facies 4 sandstone units. Photo was taken at MS#1, 49 m above base. D) Syneresis cracks on a sandstone bed base. Photo was taken south of MS#1, 53 m above basal bentonite.
See Fig.7 for section locations & Appendix 2 for graphic logs. Hammer is 28 cm tall.

Facies 5

Description

Facies 5 consists of amalgamated, sharp-based sandstone bodies (Fig 10A). Sandstone beds are mostly fine- to medium-grained. The sandstone beds are of three types: 1. Those containing soft-sediment deformation (SSD) features with large convolute bedding and loading casts, 2. Stratified units, with dominantly hummocky cross-stratification (HCS) and flat to low angle cross-lamination, 3. rotated masses with a variety of structure and showing growth faulting in places (Fig. 10 B-F). Observed sedimentary structures include large-scale hummocky cross-stratification (HCS), flat to low-angle cross-lamination, ripple cross-lamination, convolute bedding, loading, and trough cross-bedding. The sandstones contain large syneresis cracks and gutter casts on their bases. Wave ripples and interference wave ripples are common on sandstone beds tops. Facies 5 includes chaotic sandstone-filled incised gullies that are up to 6m deep. Bioturbation in the sandstones is variable, but shows generally low to moderate intensities (BI= 0-3). Observed traces include *Planolites, Diplocraterion, Teichichnus, Thalassinoides, Cylindrichnus, Lockeia, Ophiomorpha, Taenidium,* and navichnia. The trace fossils mostly are small in size, and some beds show low diversity of burrows with one or two ichnogenera. Other beds, however, show higher diversity of trace fossils with up to four different ichnogenera. The sandstone bodies thicken up-section, and are separated by thin recessive units leading to coarsening upward cycles. Beds generally thin in a strike direction from 7 m to 0.3 m. In a depositional dip direction, the beds show lateral continuity over the study area.

Interpretation

Thick, amalgamated sandstone beds indicate a more proximal depositional environment than Facies 4. Thick sandstone beds, with large-scale HCS indicate a high-energy environment of deposition. Facies 5 contains features that suggest influence from river input. Unidirectional, combined flow, and oscillatory conditions indicate deposition from outflow and reworking of sediments by waves/storms (Hunter & Clifton, 1982; Southard et al., 1990; Arnott & Southard, 1990; Dumas et al., 2005). Sandstone beds were deposited under high sedimentation rates with homopycnal outflows (friction-dominated) resulting in erosional bed bases (Fielding, 2010). Rapid deposition commonly resulted in soft-sediment deformation features (including loading and convolute bedding), and formation of fluid muds that generated soupground substrates (MacEachern et al., 2005). The muddy substrate was fluidal and susceptible to rotational failures due to sediment loading; this is evident by the presence of rotated bodies, where some of these failures developed into growth faults (Fielding, 2010). Bioturbation is present in some intervals, while other sandstone bodies are largely unburrowed. Low to moderate bioturbation (BI= 0-3) in sandstone beds indicates environmental stresses acted on these rocks during deposition. Observed ichnogenera indicates a proximal expression of the *Cruziana* Ichnofacies (MacEachern & Bann, 2008). The stressed trace fossil suite observed in some beds indicates a periodically brackish environment. This interpretation is also supported by the presence of syneresis cracks, which reflect clay shrinkage associated with salinity changes (MacEachern et al., 2005). Organisms exploit the substrate between periods of deposition, usually during fair weather conditions (Bann & Fielding, 2004; MacEachern et al., 2005). Facies 5 is interpreted to represent deposition in a proximal delta front environment under river, wave and storm influence.

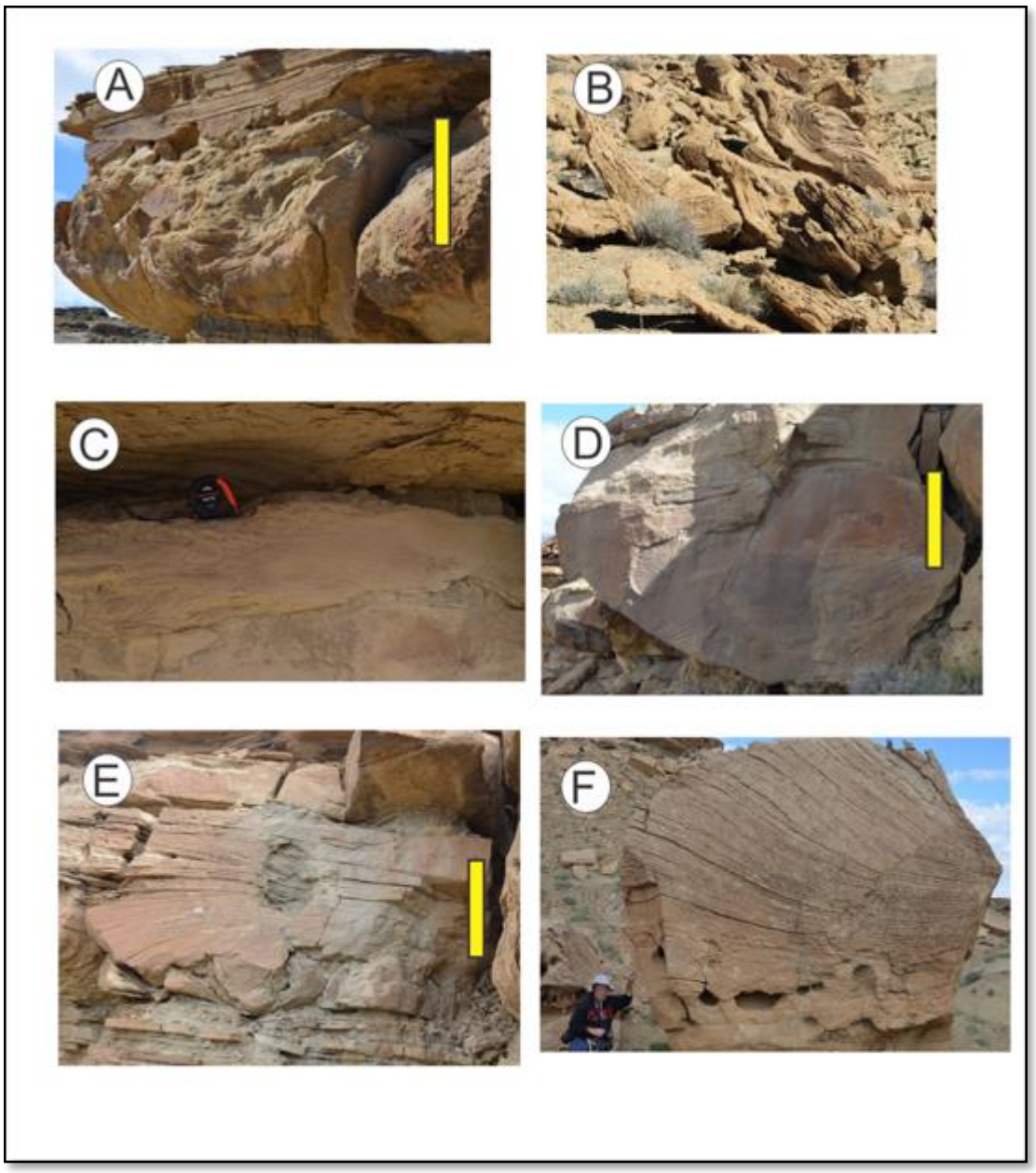

Figure 10: Photographs showing characteristics of Facies 5 (proximal delta front) observed in the study area. A) View of Facies 5 showing convolute bedding at the base and stratified top. Photo was taken at MS#3, 34 m above base. Yellow bar is 3 m. B) View of soft-sediment deformation (SSD) features observed in Facies 5. Photo was taken at MS#10, 73 m above base. C) Stratified (HCS) nature of Facies 5. Photo was taken at MS#1, 54 m above base. Tape measure height is 12 cm. D) Rotated sandstone body observed within Facies 5. Photo was taken around 60 m above basal bentonite bed. Yellow bar is 1 m. E) Growth faulting seen in Facies 5. Yellow bar is 2m. F) A fallen block showing rotation and displacement of beds within a growth fault hangingwall. See Fig.7 for section locations & Appendix 2 for graphic logs.

FACIES STACKING PATTERNS

Vertical measured sections show generally thickening and coarsening upward trends. Sandstone thickens up-section at the expense of siltstone and claystone. The sections show, in general, a change from basal shales, through interbedded siltstone and sandstone, to amalgamated and trough cross-bedded sandstones (Fig. 11). This vertical transition in facies from offshore marine to prodelta and then delta front facies indicates deltas prograding into an offshore environment (Plint, 1988; Bhattacharya, 2010).

Sediment delivery to distal localities likely occurred during significant relative sea-level falls. Incision and downcutting into underlying distal deltaic facies at multiple horizons suggest several delta progradational cycles and predominantly falling-stage accumulation. The lack of topset packages above the delta front deposits indicates deposition under forced regression (Catuneanu, 2006). Sharp-based sandstone bodies also indicate falling-stage accumulation (Plint & Nummedal, 2000). Therefore, stacking pattern and incision in the study area are consistent with deposition under falling-stage accumulation.

GULLY FILLS

In the study area, three incised gully fills were recognized within the described succession (Fig. 12). These gully fills occur at different stratigraphic horizons. Identification of incised gullies was based on field observation, detailed measured sections, mapping, and stratigraphic positioning. A series of canyons cut the outcrop, mainly in a SW-NE direction, allowed the mapping of the gully fills and recognition of

their geometries. In this paper, recognition of incised gully fills is based on criteria

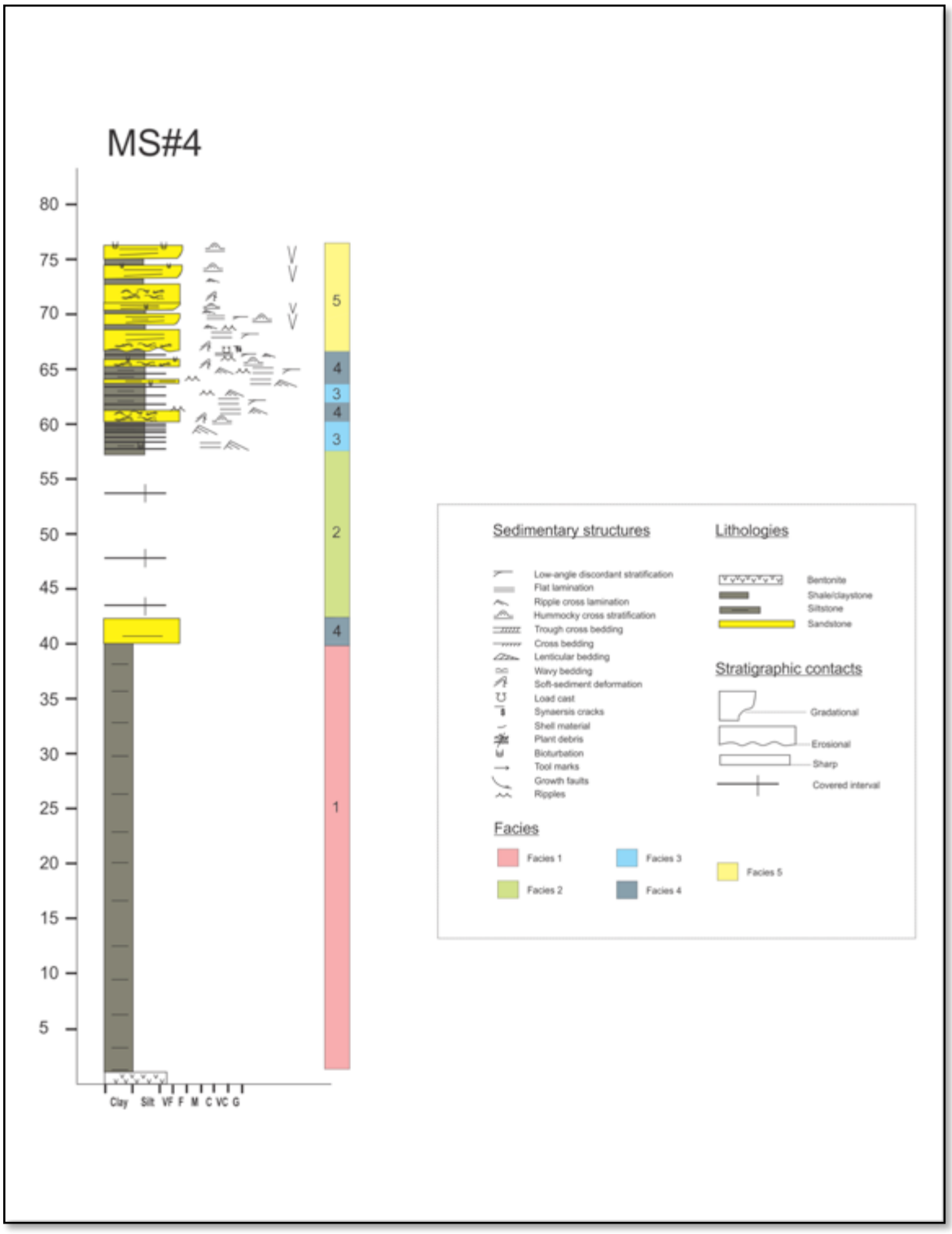

Figure 11: Measured section #4 showing how facies stack in a vertical succession.

presented by Zaitlin et al. (1994) which include: (1) The gullies show a negative (erosional) topographic feature that cuts into interbedded sandstone and siltstone, and are filled by sandstone deposits. The bases of the gullies truncate earlier deposits. (2) The base of the gully fills exhibit a juxtaposition of more proximal facies over more distal deposits, which is known as basinward shift in facies according to Van Wagoner et al, (1990). Incised gullies are morphologically similar to incised valleys but differ in size and in the environmental context; the gullies are smaller than valleys, and are formed and filled entirely within a subaqueous, delta front setting.

Description

The incised gully fills are elongate bodies in a NW-SE direction, with their margins extending to the east and west. The gully fills widen downdip (SE). They are up to 6 m deep and 300 m wide. Three gully fills in different stratigraphic horizons were recognized, and they are named in this paper from lower to upper: GF1, GF2, and GF3 (Fig. 13). The lower gully fill, GF1, cuts through interbedded siltstones and sandstones of distal front facies and is up to 4 m thick (Fig. 14a). GF1 is filled with very fine- to fine-grained sandstone that shows soft-sediment deformation and/or stratification. Stratification in GF1 includes flat to low-angle cross-lamination and ripple cross-lamination. The middle gully fill, GF2, is the thickest and widest (6m deep and 300m wide) (Fig. 14b). The western edge of GF2 is not clearly defined, as the outcrop does not extend all the way to the west, while the eastern edge can be defined. GF2 is filled with deltaic fine- to medium-grained sandstones of proximal delta front facies. The middle gully fill has a lower story and an upper story. The basal story is chaotic, convolute

bedded, or massive, while the upper story is stratified (Fig. 14c). Gutter casts are common at the base of the gully fill. The lower story shows loading, contains silt clasts and plant debris, and, locally, rotated with growth faulting. Profound soft-sediment deformation (SSD) features are seen in the lower story of the gully fills. Common large synaeresis cracks can be seen around the margins of the lower story fill. The lower story has a limited width, while the upper story (i.e. stratified part) extends as wings in an E-W direction. The east and west margins of the gully fill show gradual pinchouts (wings) with the thickest part of the fills in the middle. The upper, stratified story shows flat to low-angle cross-lamination and trough cross bedding. The upper gully fill (GF3) is the thinnest, with a maximum thickness of 3 m. It also shows a two-story division; with the lower story convolute bedded, loaded, and the upper story stratified. Large syneresis cracks and sole marks can be seen on the base of the fill.

Interpretation

Incised valleys and gullies usually result from fluvial erosion during relative fall in sea level (Van Wagoner et al., 1990; Allen & Posamentier, 1993; Willis, 1997). Fluvial deposits incising into offshore shelf deposits cause an abrupt facies break, which argues for relative sea-level fall. When rivers incise due to relative sea-level fall, they usually truncate earlier highstand strata (Plint & Nummedal, 2000). Having been cut, valleys are said to fill during sea-level stillstand and subsequent rise (Posamentier and Vail, 1988; Posamentier et al., 1988; Van Wagoner et al., 1990; Zaitlin et al., 1994). Recently, experimental studies and outcrop studies from Quaternary deltas have offered an alternative view of incised valley evolution. These studies show that paleovalleys are the

final product of continuous erosion, valley widening, and deposition (Martin et al., 2011; Blum et al., 2013). Strong and Paola (2008) used experimental data to show that erosion and deposition continually change the shape of an incised valley during valley incision and filling, and after valley filling rather than being a continuous process of excavation. Blum et al. (2013) argue that periods of incision are associated with minimal sediment export, and the increased flux of sediments to river mouths is associated with valley widening.

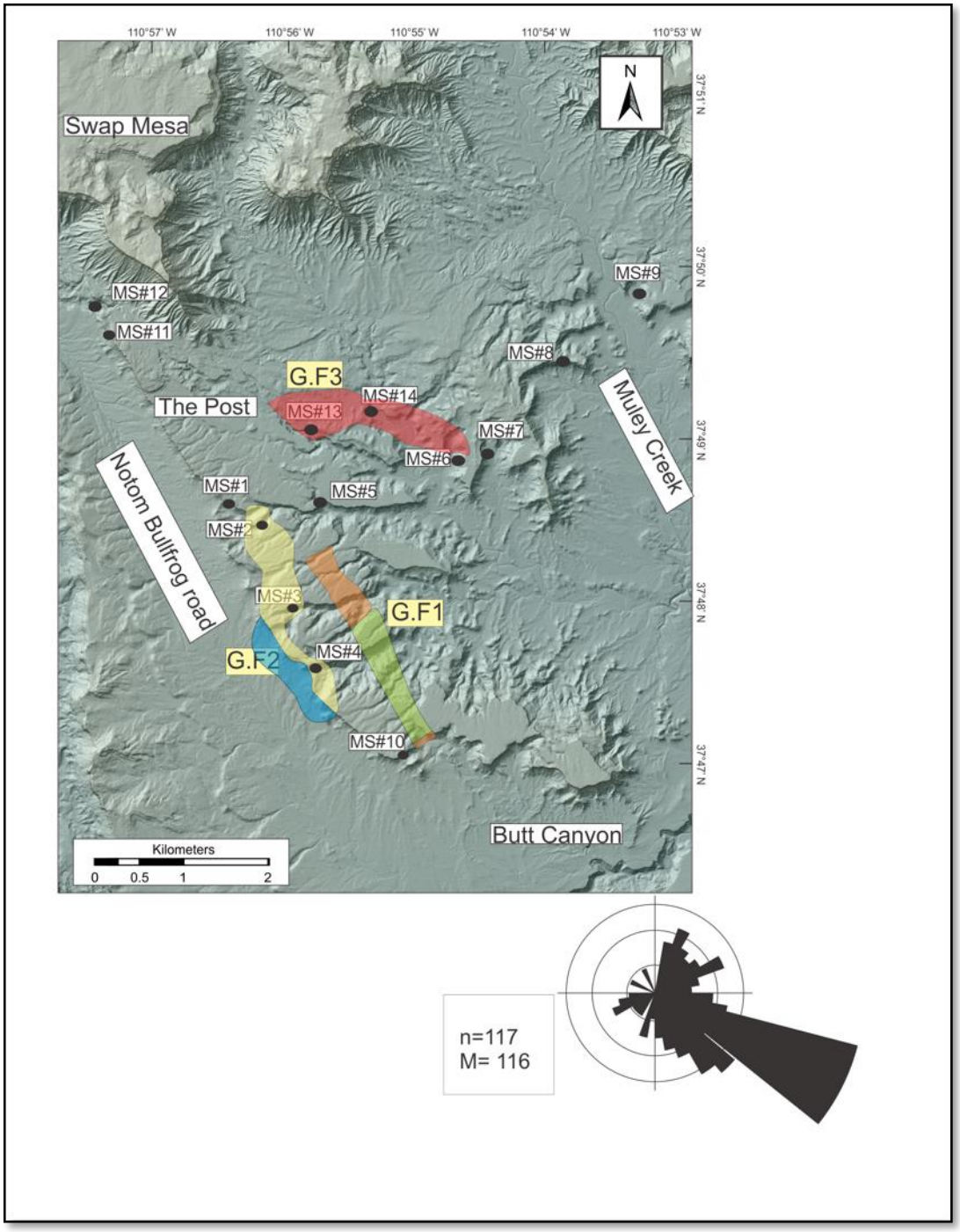

Figure 12: Map of the study area showing three gully fills mapping. Note the paleocurrent data indicate SE sediment dispersal. The lower gully fill is shown in orange and green; where green color represents area where gully fill was not observed, but inferred from continuity to the SE. The middle gully fill is shown in yellow and blue; where blue color indicates extrapolation of continuity of the gully fill, as the western side is not defined over that area. The upper gully fill is represented by red color.

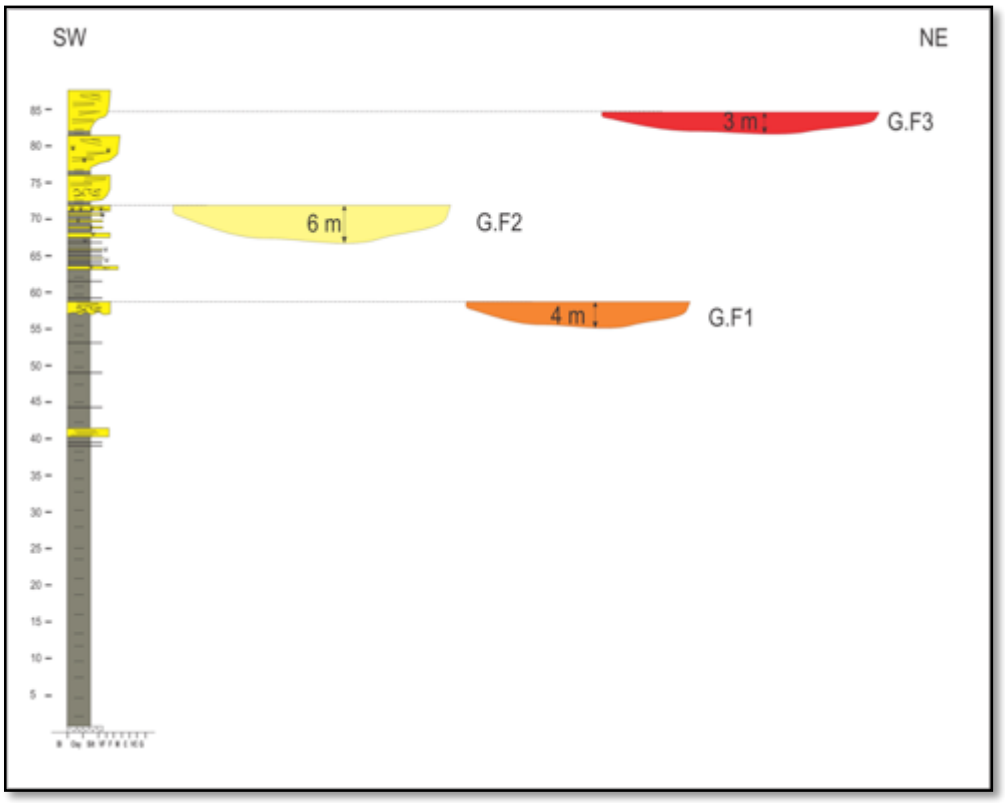

Figure 13: Schematic illustration of the three gully fills in depositional strike direction, showing their thickness and stratigraphic positions. The lower gully fill (GF1), middle gully fill (GF2), and the upper gully fill (GF3) are shown.

Zaitlin et al. (1994) explained that the facies filling incised valleys depend mainly on the position along the valley profile. They divided valleys into three segments: seaward reach, middle reach, and innermost reach, and argued that each segment of the valley is composed of specific facies. Willis (1997) illustrated that facies within incised valleys are related largely to the rate of sea-level rise, which affects accommodation and sediment supply. He explained that rapid sea-level rise will flood the incised valley and sediment supply will be insufficient to keep up, which will cause the incised valley to

form an estuary. The resulting facies within the valley will be a thin sheet of fluvial deposits, which will be capped by muds depositing from suspension, which he called "flood based" valleys. In contrast, slow sea-level rise creates accommodation in the incised valleys in a pace that sediment supply can keep up with. This means that the valleys are filled before they are flooded and preserved facies within the valley will be fluvial, "flood-capped" valleys.

The erosional contact at the base of the gully fills in the study area is interpreted as a product of relative sea-level fall by the same argument, although in this case the gully fills are composed of proximal delta front deposits incised into medial or distal delta front facies. Erosional surfaces at the base of these gully fills indicate a basinward shift in facies.

In the study area, presence of gully fills in three different stratigraphic positions indicate downcutting and sea-level drawdown. Stacking patterns and gully fills indicate at least three episodes of progradation and erosional downcutting. Each gully fill is therefore associated with a drawdown in relative sea level. As the sea level was falling, the river supplying sediment to the delta front adjusted to this drawdown by extending seaward, leading to the incision of gullies that truncated previously deposited distal delta front facies. Migrating channels filled the lower part of gully fills depositing massive (amalgamated) sandstone with high sedimentation rates that resulted in SSD and convolute bedding. As the flow or flows decelerated, the stratified top story was deposited on top of the massive sand and along the flanks as wings. The gullies were filled by more proximal facies than the underlying facies that the gullies cut into. This

means that the filling of the incised gullies was not during transgression. The filling of gullies by proximal delta front facies indicate basinward shift in facies. Therefore, the gully fills were cut and filled during falling-stage and lowstand prior to transgression. Controls on sea level cyclicity are discussed later in the document in the sequence stratigraphy section.

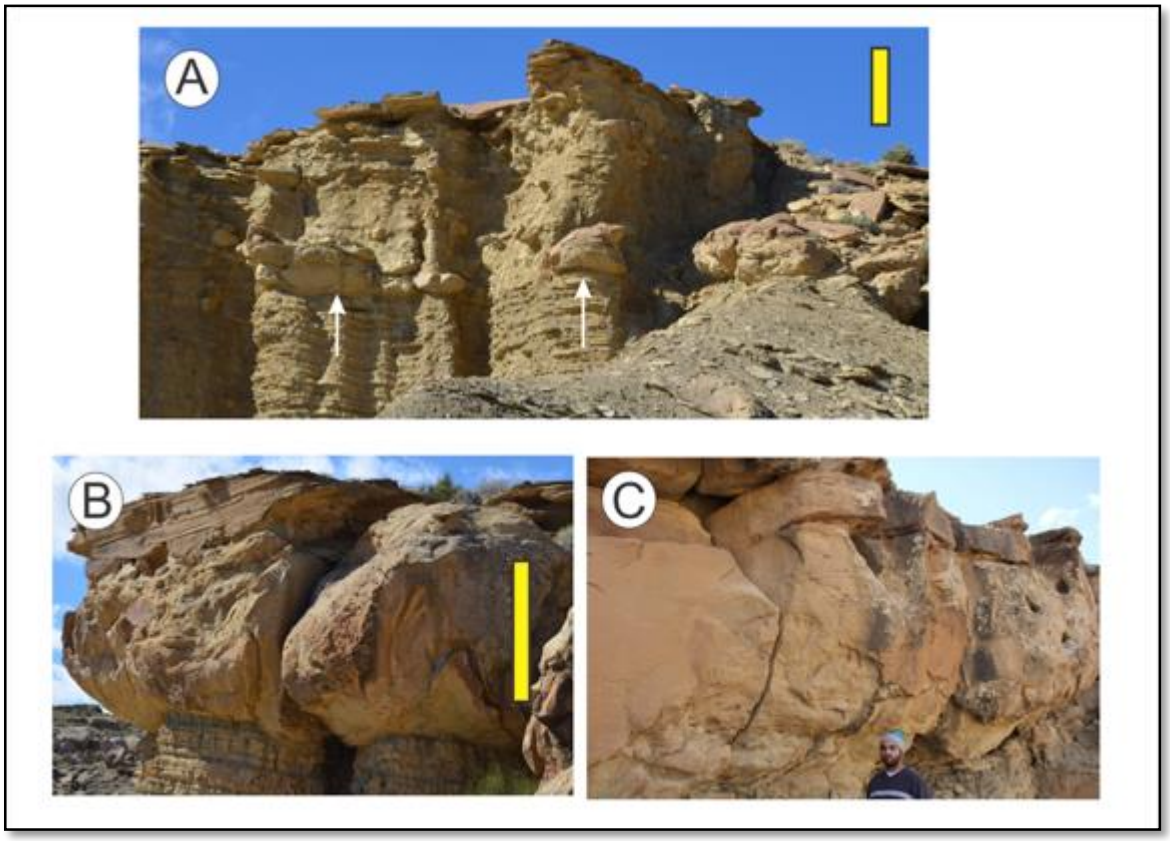

Figure 14: Photographs showing different characteristics of gully fills in the study area. A) The lower gully fill (GF1), note sandstone bodies sticking out of interbedded sandstone and siltstone (white arrows). Photo was taken around 50 m above basal bentonite. Yellow bar is 3 m. B) Photo of middle gully fill (GF2) taken at MS#3, 34 m above base of measured section. The photo shows the lower chaotic part and the upper stratified part. Yellow bar is 3 m. C) Photograph showing the lower and upper stories of GF2. Photo was taken around 58 m above the basal bentonite.
See Fig.7 for section locations & Appendix 2 for graphic logs

DEPOSITIONAL ENVIRONMENT

Facies stacking patterns and lateral variations in facies assemblages observed throughout the Ferron Sandstone in the study area show evidence for repeated shallow marine deltaic progradational events (Figs. 11, 16). Shallow marine deposits commonly display varieties of structures due to waves, storms, tidal currents, river influence, and marine processes, with typically one process dominating (Hampson et al., 2008). Sedimentary structures observed within the Ferron Sandstone in the study area suggest that it was the product of fluvial and wave-influenced deltaic systems. Various sedimentary structures form evidence of fluvial influence in the Ferron deposits. The presence of current ripples and combined-flow ripples indicate deposition under unidirectional flow and combined current-wave regimes. High sedimentation rates during river floods, indicated by soft-sediment deformation (SSD), also show that fluvial influence was evident. Stressed trace fossils (Facies 4 &5) and syneresis cracks also support the notion of frequent effluxes of fresh water into a marine water body, and therefore a fluvial influence. Evidence for storm waves can be seen by the presence of hummocky cross-stratification (HCS), trough-cross bedding, and flat- to low-angle lamination in combination with a decreasing siltstone ratio up section. Storm waves would disperse sand in the proximal delta front environment and carry the muds away in suspension. The muds would be transported to more distal locations and dropped in an offshore environment from suspension later on. The shallow sea floor was mud-rich at the time of the Ferron sandstone deposition. The rapid sedimentation of the sand resulted in delta front slope failures, and formation of rotated sand masses.

Paleocurrent data from delta front deposits in the study area indicate southeastward delta progradation (Fig. 12). The regional paleocurrent dataset for the Ferron Sandstone has an eastward mode (Fielding, 2010), which means that the paleoshoreline was oriented north-south and deltas prograded to the east. This indicates that the delta front facies show an element of longshore progradation. Such progradation could be due to geostrophic deflection of outflow southward by winds (Fielding, 2010) (Fig.15). The delta prograded into shallow sea along gently dipping slopes, which is indicated by the absence of high-angle clinoforms.

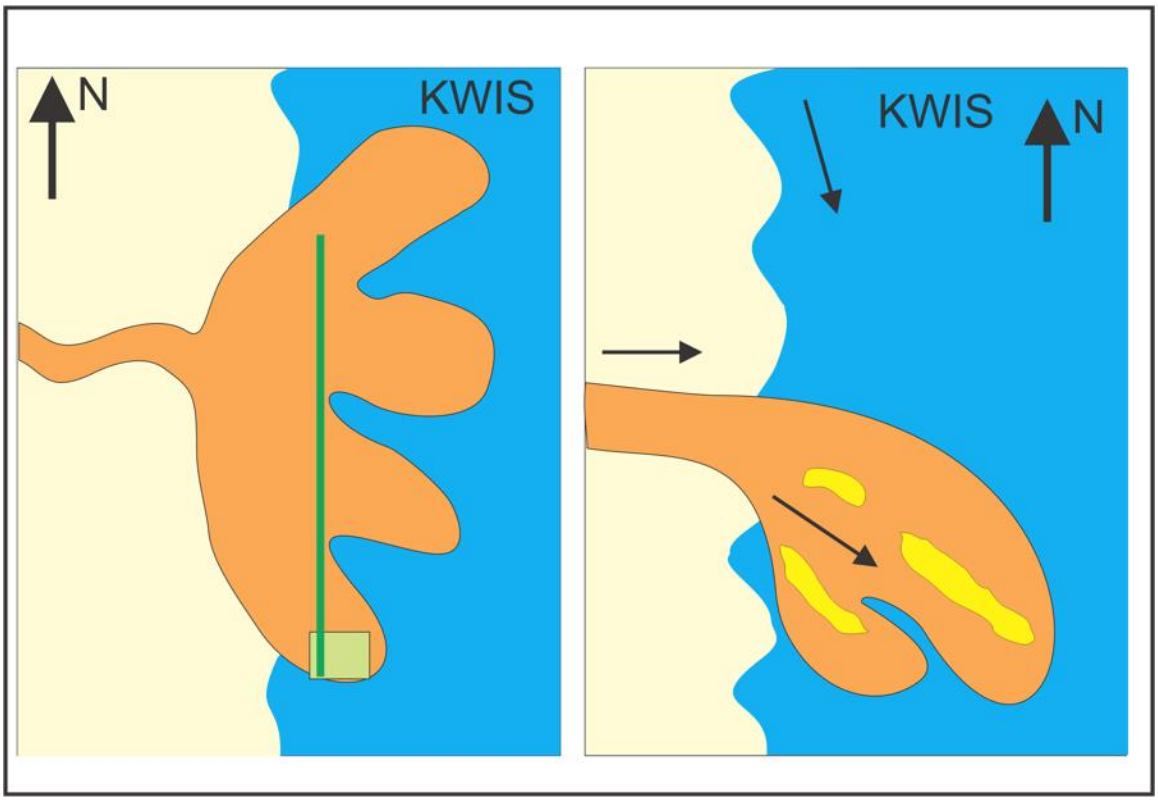

Figure 15: Diagram illustrating in a plan-view explaining the paleocurrent distribution observed in the Ferron Notom deltaic deposits. Sediment is dispersed into water in an east direction, and then diverted by oblique winds that resulted in a southeastward paleocurrent mode in delta front deposits. The green line represents the regional cross section (Fig. 2) over 67 km and the box denotes the study area, which is expanded in the diagram to the right. The yellow shapes represent the observed gully fills in delta front deposits.

SEQUENCE STRATIGRAPHY

The regional sequence stratigraphy of the Ferron Sandstone in the study area is incompletely documented. Mapping of the Ferron Sandstone exposures along the western limb of the Henry Mountains was carried out by Fielding (2011) (Fig. 2), where regional sequence stratigraphy is needed to understand these rocks more thoroughly. This study adds to the understanding of the regional sequence stratigraphy of the Notom delta complex. This section will provide an account of the sequence stratigraphy of the Ferron Sandstone in the study area in terms of parasequences, key stratigraphic surfaces, and systems tracts.

Parasequences

A parasequence is defined as " a relatively conformable, genetically related succession of beds or bedsets bounded by marine-flooding surfaces or their correlative surfaces" (Van Wagoner et al., 1990; Kamola & Van Wagoner, 1995; Catuneanu, 2006). Parasequences are the building blocks of sequences, and in outcrops, they show a shallowing and coarsening upward character (Van Wagoner et al., 1990). A parasequence boundary is defined by a flooding surface that indicates increase in water depth and landward shift in facies (Van Wagoner et al., 1990; Kamola & Van Wagoner, 1995). The flooding surface is indicated by deeper water facies sharply overlying shallower facies.

Vertical measured outcrop sections in the study area show multiple shallowing- and coarsening-upward parasequences, and key stratigraphic surfaces, within the Ferron Sandstone lower member (Figs. 16; 17, and 18). Vertical trends show shallowing up from

basal offshore marine mudrocks to proximal delta front facies recording fluvial, wave, and storm influence on prograding deltaic strata. As many as four parasequences were observed in measured sections (Fig. 16). The parasequences have sharp and erosional, to locally gradational, bases. The overall stacking pattern of these parasequences and the gently dipping clinoforms within the proximal delta front facies suggest a prograding delta under limited accommodation. Coarsening-upward successions have bioturbated tops with bioturbation index (BI) of 0 – 1. Recognized traced fossils include *Ophiomorpha, Diplocraterion, Taenidium and Cylindrichnus.*

Systems Tracts

Facies stacking patterns and the presence of three incised gully fills suggest several delta progradational cycles and accumulation predominantly during falling stage. Thin, sharp-based sandstone bodies within shelf deposits in general indicate periods of relative sea level fall with limited accommodation (Plint, 1988; Plint & Nummedal, 2000). Such deposits are in many cases isolated and encased in offshore marine mudstones. The sediment was delivered to distal localities likely during significant sea level drawdowns. Incision and downcutting into underlying distal deltaic facies at multiple horizons in the study area indicate at least three episodes of forced regression. Forced regressive deposits within the Ferron Sandstone have been described to the north of the study area within the same succession (Li et al., 2011 a,b; Zhu et al., 2012). The lack of high-angle clinoforms within the proximal deltaic sandstones suggests low accommodation conditions. Therefore, the deposition within the Ferron Sandstone in the study area is considered to be accommodation-driven (cf. Porebski & Steel, 2006).

Facies stacking patterns indicate deposition within falling-stage delta progradation. Outcrop measured sections show progradational sandstone bodies with no preservation of a delta plain topset, which is an indicator of forced regression (Fig. 16, 17, and 18). Normal regression typically is accompanied by aggradation and progradation, while the forced regression is marked by fluvial downcutting with no aggradation (Posamentier & Morris, 2000; Catuneanu, 2006). The presence of sharp-based delta front sand bodies in the study area is another indicator of forced regression (Fig 9B). Their presence is indicative of missing facies, and could be linked to erosion by relative sea-level fall (Plint 1988; Posamentier & Morris, 2000). A significant sea level fall results in fluvial downcutting and incision (Posamentier et al., 1988; Plint & Nummedal 2000; Catuneanu, 2006). Thus, the presence of three gully fills in the study area indicates episodes of sea level drawdown. The depositional dip cross-section, however, does not show a descending regressive trajectory (Fig. 17).

Placement of the sequence boundary within falling-stage strata is still debated with two competing definitions. Posamentier and Morris (2000) placed the sequence boundary at the base of the first erosion surface that is formed by wave reworking during relative sea-level fall. Plint and Nummedal (2000), however, defined the sequence boundary at the top of forced regressive deposits, which corresponds to a subaerial unconformity. Posamentier and Morris (2000) definition of the sequence boundary proved to be problematic. It is difficult to recognize this surface in outcrops, core, or wireline logs (Catuneanu, 2006). There are also complications in placing this surface along the shelf and in its correlative conformity. Therefore, in this study, the latter definition of sequence boundary is preferred (Fig. 16). This surface is also a flooding

surface that is topped by marine shale. Hence, the SB/FS is placed on top of the delta front facies.

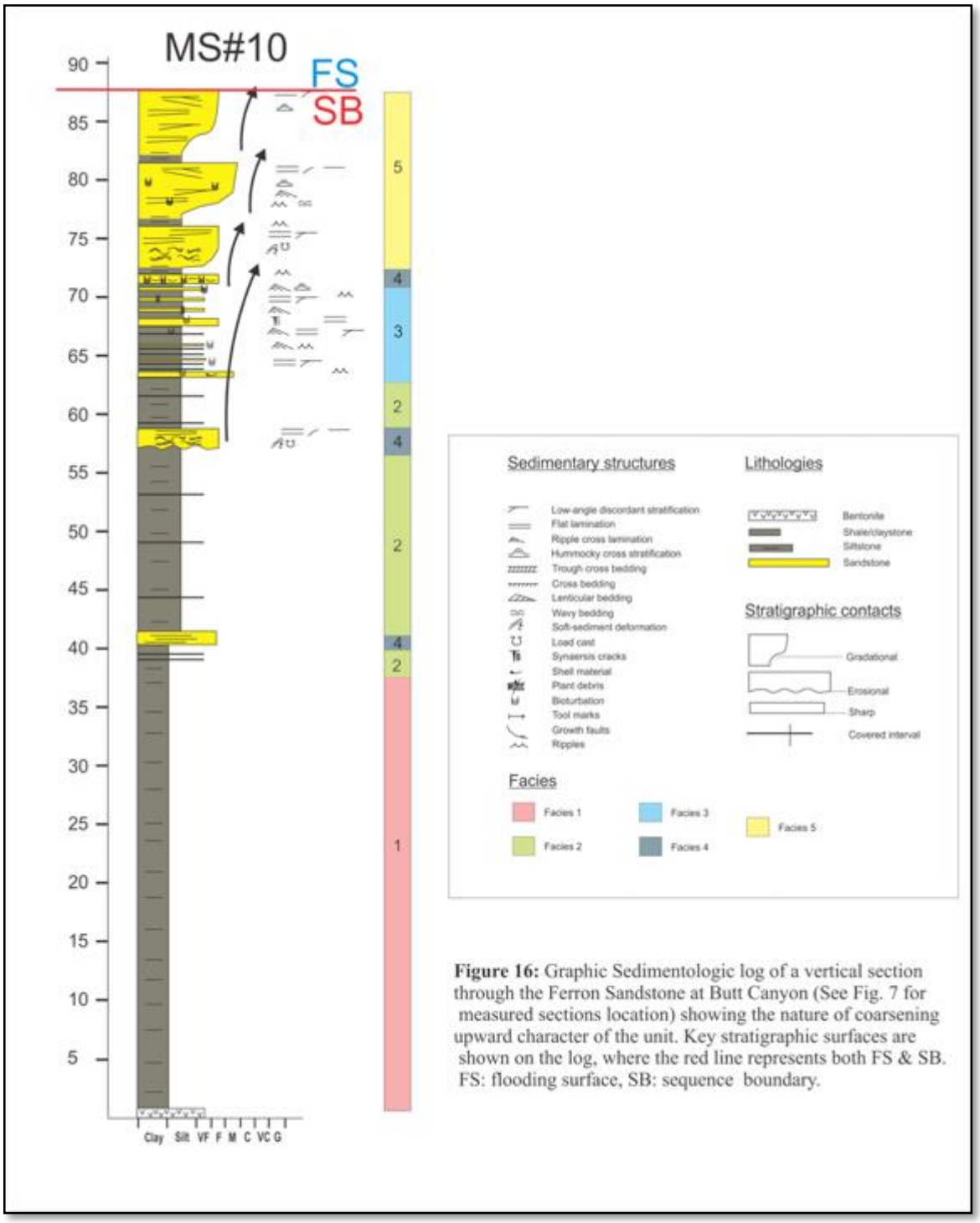

Figure 16: Graphic Sedimentologic log of a vertical section through the Ferron Sandstone at Butt Canyon (See Fig. 7 for measured sections location) showing the nature of coarsening upward character of the unit. Key stratigraphic surfaces are shown on the log, where the red line represents both FS & SB. FS: flooding surface, SB: sequence boundary.

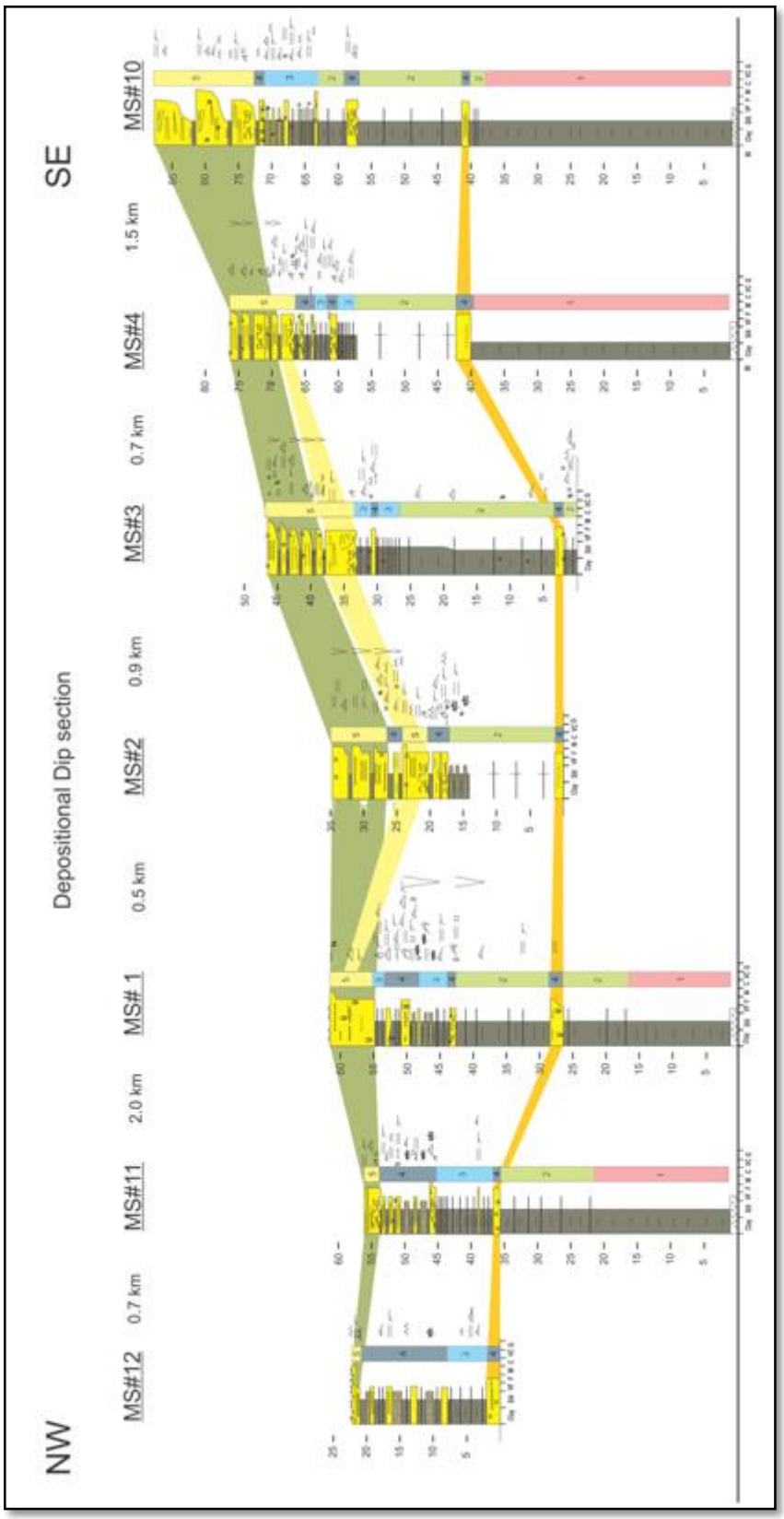

Figure 17: Depositional dip cross section. The change in thickness of prograding cycles show thickening in depositional dip (SE) direction instead of the expected thinning.

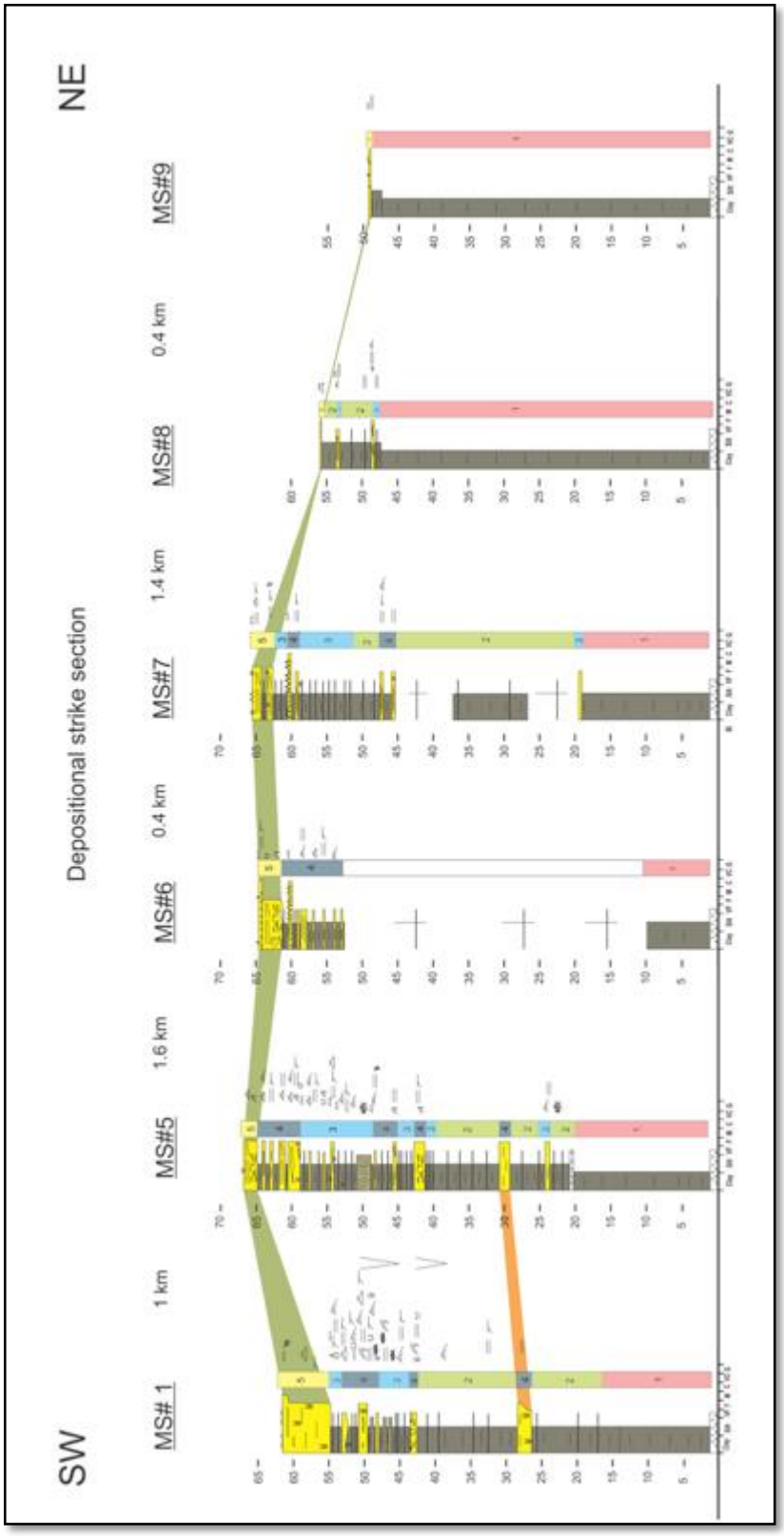

Figure 18: Depositional strike cross section. . The change in thickness of prograding cycles shows flank thinning of the delta lobe

CONTROLS ON CYCLICITY

In this section, controls on sea level fall that resulted in prograding delta deposits and gully fills are discussed. Allogenic controls such as tectonics, eustasy, and climate change are responsible for cyclic depositional patterns in the rock record in general. Autogenic controls such as shoreline autoretreat and delta lobe switching are also important controls of cyclicity.

The Ferron Sandstone was deposited in an active foreland basin, which suggests that tectonic activity is a possible control on cyclicity. Fielding (2011) showed that tectonic forcing resulted in a structural arch within the Ferron Sandstone, related to forebulge growth. This supports the view that tectonic effects had a dominant influence on the stratigraphy of the Cretaceous Western Interior Seaway. Zhu et al. (2012), using geochronological data, showed relative falls of sea level corresponding to Milankovitch frequencies. They hypothesized that glacio-eustacy is the dominant control on the cyclicity of Ferron deposits. Climatic changes also can affect cyclicity and result in shoaling-up parasequences with bounding flooding surfaces (Van den berg van Saparosa & Potsma, 2008). Climate controls the sediment supply to the basin. Large sediment volumes can be delivered into the basin by large storms, which would initiate high discharge events.

During the deposition of the Ferron Sandstone, more than one controlling factor was likely responsible for the observed cyclicity. The depositional context, within an active foreland basin, indicates that tectonic effects would be a major control. Eustasy is another proposed control as suggested by the geochronological analysis of Zhu et al. (2012). Climatic controls affect the sediment supply to the basin, which in turn, controls

deposition. Therefore, multiple allogenic controls influenced the deposition and preservation of the Ferron Sandstone.

CONCLUSIONS

The Turonian Ferron Sandstone Member of the Mancos Shale accumulated in a foreland basin by deltas prograding eastward into the Cretaceous Western Interior Seaway. A detailed stratigraphic study of one component deltaic unit within the Ferron Sandstone outcrop in south-central Utah allowed recognition of facies stacking patterns, sequence stratigraphy, and depositional environment interpretations. Observed facies include fine-grained mudstones (offshore), mudstone with thinly interlaminated sandstone (prodelta), thinly interbedded siltstones and fine-grained sandstones (distal delta front), thickly interbedded siltstones, coarse-grained siltstones and fine-grained sandstones (medial delta front), and amalgamated fine-to medium-grained sandstones (proximal delta front). Vertical measured sections show change from offshore marine mudstones, through interbedded siltstone and sandstone, to amalgamated and trough cross-bedded sandstones. Facies in the study area indicate progradation of deltas into offshore environments under low accommodation. The observed sedimentary structures within the studied interval indicate fluvial and wave influences on broadly deltaic deposits.

Three gully fills in different stratigraphic positions were observed, mapped, and described. The gully fills are up to 6 m deep and 300 m wide. The basal parts of these gully fills preserve convolute bedding, rotational failures and growth faults. The presence of these gully fills suggests episodes of delta progradation and sea level drawdown.

Detailed description of the gully fills led to the interpretation that they were cut and filled during sea level fall, and not during transgression.

The paleoshoreline was oriented north-south and the deltas prograded into the east depositing the Ferron sandstone (Fielding, 2010). Paleocurrent data within delta front facies in the study area indicate southeast sediment dispersal. Sediments were deflected in a south-southeastward direction as a result of the Coriolis Effect upon prevailing winds and water currents upon entering the KWIS. The facies stacking pattern and the lack of delta plain topset argues for deposition within falling-stage systems tracts. Incision and downcutting into underlying distal deltaic facies also support the falling-stage interpretation. The depositional dip cross-section, however, does not show a descending regressive trajectory. Forced regression is implied by facies associations and incision, despite the lack of descending regressive trajectory in the depositional dip direction.

References

Allen, G.P., and Posamentier, H.W. (1993) Sequence stratigraphy and facies model of an incised valley fill: the Gironde estuary, France: Journal of Sedimentary Petrology, 63: 378–391.

Arnott, R.W.C. and Southard, J.B. (1990) Exploratory flow-duct experiments on combined-flow bed configurations, and some implications for interpreting storm-event stratification: Journal of Sedimentary Research, 60: 211 – 219.

Bann, K.L. and Fielding, C.R. (2004) An integrated ichnological and sedimentological comparison of non-deltaic shoreface and subaqueous delta deposits in Permian reservoir units of Australia; in McIlroy, ed., The application of ichnology to paleoenvironmental and stratigraphic analysis: Geological Society of London Special Publication, 228: 273 – 310.

Bann, K.L., Tye, S.C., MacEachern, J.A., Fielding, C.R., and Jones, B.G. (2008) Ichnological and sedimentological signatures of mixed wave- and storm-dominated deltaic deposits: examples from the early Permian Sydney Basin, Australia *in* Recent advances in models of siliciclastic shallow-marine stratigraphy: Hampson, G.J., Steel, R.J., Burgess, P.M., and Dalrymple, R.W., *eds*.: Society for Sedimentology Special Publication, 90: 293 - 332.

Bhattacharya, J.P. and Davies, R.K. (2004) Sedimentology and structure of growth faults at the base of the Ferron Member along Muddy Creek, Utah *in* Regional to Wellbore Analog for Fluvial– Deltaic Reservoir Modelling: The Ferron Sandstone of Utah: Chidsey, T.C., Adams, R.D., and Morris, T.H., *eds*.: American Association of Petroleum Geologists, Studies in Geology, 50: 279 – 304.

Bhattacharya, J.P. and Tye, R.S. (2004) Searching for modern Ferron analogs and application to subsurface interpretation *in* Regional to Wellbore Analog for Fluvial– Deltaic Reservoir Modelling: The Ferron Sandstone of Utah: Chidsey, T.C., Adams, R.D., and Morris, T.H., *eds*.: American Association of Petroleum Geologists, Studies in Geology, 50: 39–57.

Bhattacharya, J.P. and MacEachern, J.A. (2009) Hyperpycnal rivers and prodeltaic shelves in the Cretaceous seaway of North America: Journal of Sedimentary Research, 79: 184 – 209.

Bhattacharya J.P. (2010) Deltas *in*: Facies Models 4: Dalrymple, R.G. and James, N.P., *eds*.: Geological Association of Canada, 6: 233-264.

Blum, M.D. and Tornqvist, T.E. (2000) Fluvial responses to climate and sea-level change: a review and a look forward: Sedimentology, 47: 2 – 48.

Blum, M.D. and Aslan, A. (2006) Signatures of climate vs. sea-level change within incised valley-fill successions: Quaternary examples from the Texas Gulf Coast: Sedimentary Geology, 190: 177–211.

Blum M., Martin J., Milliken K., and Garvin M. (2013) Paleovalley systems: Insights form Quaternary analogs and experiments, Earth-Science Reviews: 116, 128-169.

Bon, R.L. (2005) Coal resources of state-owned lands in the Muley Canyon Sandstone Member of the Mancos Shale, Henry Mountains Coalfield, Wayne and Garfield Counties, Utah: unpublished report for Utah School and Institutional Trust Lands, Utah Geological Survey, online: http://trustlands.utah.gov/download/mining/HenryMountains.pdf

Blakey, R.C. URL: http://jan.ucc.nau.edu/~rcb7/index.html

Catuneanu, O. (2006) Principles of sequence stratigraphy: Elsevier: 375 pp.

Catuneanu, O., Abreu, Bhattacharya, J., Blum, M.D., Dalrymple, R.W., Eriksson, G., Fielding, C.R., Fisher, W.L., Galloway, W.E., Gibling, M.R., Giles, K.R., Holbrook, J.M., Jordan, R., Kendall, C.G.St.C., Macurda, B., Martinsen, O.J., Miall, A.D., Neal, J.E., Nummedal, D., Pomar, L., (2009) Towards the standardization of sequence stratigraphy: Earth-Science Reviews, 92: 1–33.

Chidsey T.C. Jr. (2001) Geological and petrophysical characterization of the Ferron Sandstone for 3-D simulation of a fluvial-deltaic reservoir: Report of Utah Geological Survey, Salt Lake City, Utah: 490 pp.

Chidsey, T.C., Adams, R.D., and Morris, T.H., eds., (2004) Regional to Wellbore Analog for Fluvial–Deltaic Reservoir Modelling: The Ferron Sandstone of Utah: American Association of Petroleum Geologists, Studies in Geology, 50: 568 pp.

Cotter, E. (1975) Deltaic deposits in the Upper Cretaceous Ferron Sandstone, Utah, *in* Deltas, models for exploration: Broussard, M. L. ed.,: Houston Geological Society: 471-484.

Dumas, S., Arnott, R.W.C., and Southard, J.B. (2005) Experiments on oscillatory-flow and combined-flow bed forms: Implications for interpreting parts of the shallow-marine sedimentary record: Journal of Sedimentary Research, 75: 501– 513.

Dumas, S. and Arnott, R.W.C. (2006) Origin of hummocky and swaley cross-stratification – The controlling influence of unidirectional current strength and aggradation rate: Geology, 34: 1073 – 1076.

Eaton, J.G. (1990) Stratigraphic revision of Campanian (Upper Cretaceous) rocks in the Henry Basin, Utah: The Mountain Geologist, 27: 27-38.

Enge, H.D. and Howell, J.A. (2010) Impact of deltaic clinothems on reservoir performance: Dynamic studies of reservoir analogs from the Ferron Sandstone Member and Panther Tongue, Utah: AAPG Bulletin, 94: 139 – 161.

Fielding, C.R. (2010) Planform and Facies Variability in Asymmetric Deltas: Facies Analysis and Depositional Architecture of the Turonian Ferron Sandstone in the Western Henry Mountains, South-Central Utah, U.S.A.: Journal of Sedimentary Research, 80: 455-479.

Fielding, C.R., Antia, J., Birgenheier, L.P., and Corbett, M.J. (2010) A Field guide to the Cretaceous succession of the western Henry Mountains syncline, South-Central Utah: Utah Geological Association Publication, 39: 276-316.

Fielding, C.R. (2011) Foreland basin structural growth recorded in the Turonian Ferron Sandstone of the Western Interior Seaway Basin, USA: Geology, 39: 1107–1110.

Gardner, M.H., Cross, T.A., and Levorsen, M. (2004) Stacking patterns, sediment volume partitioning, and facies differentiation in shallow-marine and coastal-plain strata of the Cretaceous Ferron Sandstone, Utah *in* Regional to Wellbore Analog for Fluvial– Deltaic Reservoir Modelling: The Ferron Sandstone of Utah: Chidsey, T.C., Adams, R.D., and Morris, T.H., *eds*.: American Association of Petroleum Geologists, Studies in Geology, 50: 95–124.

Garrison, J.R., and Van Den Bergh, T.C.V. (2004) High-resolution depositional sequence stratigraphy of the Upper Ferron Sandstone Last Chance Delta: an application of coal zone *in* Regional to Wellbore Analog for Fluvial– Deltaic Reservoir Modelling: The Ferron Sandstone of Utah: Chidsey, T.C., Adams, R.D., and Morris, T.H., *eds*.: American Association of Petroleum Geologists, Studies in Geology, 50: 125–192.

Gilbert, G.K. (1877) Report on the geology of the Henry Mountains: U.S. Geographical and Geological Survey, Rocky Mountain Region, Report: 160 pp.

Hale, L. A. (1972) Depositional history of the Ferron Formation, central Utah *in* Plateau-basin and range transition zone: Baer, J. L., and Callaghan, E., *eds*.: Utah Geological Association Publication, 2: 115-138.

Hampson, G.J., Proctor, E.J., and Kelly, C. (2008) Controls on isolated shallowmarine sandstone deposition and shelf construction: Late Cretaceous Western Interior Seaway, northern Utah and Colorado, USA *in* Recent advances in models of siliciclastic shallow-marine stratigraphy: Hampson, G.J., Steel, R.J., Burgess, P.M., and Dalrymple, R.W., *eds*.: Society for Sedimentology Special Publication, 90: 355 - 390.

Hill, R.B. (1982) Depositional environments of the Upper Cretaceous Ferron Sandstone south of Notom, Wayne County, Utah: Brigham Young University Geology Studies, 29: 59-83.

Hunt, C.B. and Miller, R.L. (1946) General geology of the region – stratigraphy, *in* Guidebook to the Geology and Geography of the Henry Mountain Region: Hunt, C.B., *eds*.: Utah Geological Society Guidebook, 1: 6-10.

Hunt, C.B., Averitt, P., and Miller, R.L. (1953) Geology and Geography of the Henry Mountains Region, Utah: U.S. Geological Survey Professional Paper, 228: 234 pp.

Hunter, R.E. and Clifton, E.H. (1982) Cyclic deposits and hummocky cross-stratification of probable storm origin in Upper Cretaceous rocks of the Cape Sebastian area, southwestern Oregon: Journal of Sedimentary Research, 52: 127 – 143.

Kamola, D.L. and Van Wagoner, J.C. (1995) Stratigraphy and facies architecture of parasequences with examples from, Spring Canyon Member, Blackhawk Formation, Utah; in Sequence stratigraphy of foreland basin deposits; outcrop and subsurface examples from the Cretaceous of North America: American Association of Petroleum Geologists Memoir, 64: 27 – 54.

Li, W.G., Bhattacharya, J.P., and Campbell, C. (2010) Temporal evolution of fluvial style within a compound incised valley, the Ferron Notom Delta, Henry Mountains Region, Utah: Journal of Sedimentary Research, 80: 529–549.

Li, W. and Bhattacharya, J.P. (2011a) Architecture and depositional proceses of a forced regressive series in the Turonian Ferron ‘‘Notom Delta,’’ southern Utah, U.S.A.: Marine and Petroleum Geology, 28: 1517–1529.

Li, W., Bhattacharya, J.P., Zhu, Y., Garza, D., and Blankenship, E. (2011b) Evaluating delta asymmetry using three-dimensional facies architecture and ichnological analysis, Ferron “Notom Delta”, Capitol Reef, Utah, USA: Sedimentology, 58: 478–507.

Li, W., Bhattacharya, J.P., and Zhu, Y. (2012) Stratigraphic uncertainty in sparse versus rich data sets in a fluvial-deltaic outcrop analog; Ferron Notom delta in the Henry Mountains region, southern Utah: AAPG Bulletin, 96: 415–438.

Lupton, C. T. (1916) Geology and coal resources of Castle Valley in Carbon, Emery, and Sevier Counties, Utah: U.S. Geological Survey Bulletin, 628: 88 p.

MacEachern, J.A., Bann, K.L., Bhattacharya, J.P. and Howell, C.D. (2005) Ichnology of deltas *in*: River Deltas- Concepts, Models, and Examples: Giosan, L. and

Bhattacharya, J.P. *eds*.: Society for Sedimentary Geology Special Publication, 83: 49–86.

MacEachern, J.A. and Bann, K.L. (2008) The role of ichnology in refining shallow marine facies models *in* Recent advances in models of siliciclastic shallow-marine stratigraphy: Hampson, G.J., Steel, R.J., Burgess, P.M., and Dalrymple, R.W., *eds*.: Society for Sedimentology Special Publication, 90: 73 –116.

Martin, J.M., Cantelli, A., Paola, C., Blum, M.D., Wolinsky, M. (2011) Quantitative modeling of the evolution and geometry of incised valleys: Journal of Sedimentary Research, 81: 64–79.

Morton, L.B. (1984) Geology of the Mount Ellen Quadrangle, Henry Mountains, Garfield County, Utah: Brigham Young University Geology Studies, 31: 67-95.

Olariu, C., Steel, R.J., and Petter, A.L. (2010) Delta-front hyperpycnal bed geometry and implications for reservoir modeling: Cretaceous Panther Tongue delta, Book Cliffs, Utah: American Association of Petroleum Geologists, 94: 819 - 845.

Peterson, F. and Ryder, R.T. (1975) Cretaceous rocks in the Henry Mountains region, Utah and their relation to neighboring regions *in* Canyon lands country: Fassett, J.E., ed.: Four Corners Geological Society 8th Field Conference Guidebook: 167–189.

Plint, A.G. (1988) Sharp-based shoreface sequences and ‘‘offshore bars’’ in the Cardium Formation of Alberta: their relationship to relative changes in sea level *in* Sea-Level Changes: An Integreated Approach: Wilgus, C.K., Hastings, C.G., Kendall, C.G., Posamentier, H.W., Ross, C.A., and Van Wagoner, J.C., *eds*.: Society for Sedimentary Geology Special Publication, 42: 357–370.

Plint, A. G. and D. Nummedal (2000) The falling stage systems tract: Recognition and importance in sequence stratigraphic analysis *in* Sedimentary responses to forced regressions: Hunt, D. and Gawthorpe, R. L. *eds*.: Geological Society of London Special Publication, 172: 1–17.

Plint, A.G. (2010) Wave- and storm-dominated shoreline and shallow-marine systems *in* Facies Model Revisited: James, N.P., and Dalrymple, R.W., *eds*.: Society for Sedimentary Geology Special Publication, 90: 167–199.

Porebski, S.J. and Steel, R.J. (2006) Deltas and Sea-level Change: Journal of Sedimentary Research, 76: 390 – 403.

Posamentier, H.W., Jervey, M.T., and Vail, P.R. (1988) Eustatic constrols on clastic deposition I —conceptual framework *in* Sea-Level Changes: An Integreated Approach: Wilgus, C.K., Hastings, C.G., Kendall, C.G., Posamentier, H.W., Ross,

C.A., and Van Wagoner, J.C., *eds*.: Society for Sedimentary Geology Special Publication, 42: 109 – 124.

Posamentier, H.W., and Vail, P.R., 1988, Eustatic controls on clastic deposition. II. Sequence and systems tract models *in* Sea-Level Changes: An Integreated Approach: Wilgus, C.K., Hastings, C.G., Kendall, C.G., Posamentier, H.W., Ross, C.A., and Van Wagoner, J.C., *eds*.: Society for Sedimentary Geology Special Publication, 42: 125–154.

Posamentier, H.W., Allen, G.P., James, D.P., and Tesson, M. (1992) Forced regressions in a sequence stratigraphic framework: concepts, examples, and exploration significance: American Association of Petroleum Geologists, 76: 1687–1709.

Posamentier, H. W. and Chamberlain, C. J. (1993) Sequence-stratigraphic analysis of Viking Formation lowstand beach deposits at Joarcam Field, Alberta, Canada *in* Sequence stratigraphy and facies associations: Posamentier, H. W., Summerhayes, C. P., Haq, B. U. and Allen, G. P., *eds*.: 469-485.

Posamentier, H.W. and Allen, G.P. (1999) Siliciclastic Sequence Stratigraphy: Concepts and Applications: Society for Sedimentary Geology, Concepts in Sedimentology and Paleontology, 7: 210 p.

Posamentier, H.W. and Morris, W.R. (2000) Aspects of the strata architecture of forced regressive deposits; in Hunt, D., and Gawthorpe, R.L., *eds*.: Sedimentary response to forced regression: Geological Society of London Special Publication, 172: 19 – 46.

Reineck, H.-E. (1963) Sedimentgefuˆge im Bereich der su¨dlichen Nordsee: Senckenbergische Naturforschende Gesellschaft, Abhandlungen: 505 p.

Ryer, T.A. (2004) Previous studies of the Ferron Sandstone *in* Regional to Wellbore Analog for Fluvial– Deltaic Reservoir Modelling: The Ferron Sandstone of Utah: Chidsey, T.C., Adams, R.D., and Morris, T.H., *eds*.: American Association of Petroleum Geologists, Studies in Geology, 50: 3 – 38.

Ryer, T.A. and Anderson, P.B. (2004) Facies of the Ferron Sandstone, East-Central Utah *in* Regional to Wellbore Analog for Fluvial– Deltaic Reservoir Modelling: The Ferron Sandstone of Utah: Chidsey, T.C., Adams, R.D., and Morris, T.H., *eds*.: American Association of Petroleum Geologists, Studies in Geology, 50: 59–78.

Smith, C. (1983) Geology, depositional environments, and coal resources of the Mt. Pennell 2 NW Quadrangle, Garfield County, Utah: Brigham Young University Geology Studies, 30: 145-169.

Southard, J.B., Lambie, J.M., Federico, D.C., Pile, H.T., and Weidman, C.R. (1990) Experiments on bed configurations in fine sands under bidirectional purely

oscillatory flow, and the origin of hummocky cross-stratification: Journal of Sedimentary Research, 60: 1 – 17.

Strong, N. and Paola, C. (2008) Valleys that never were: time surfaces versus stratigraphic surfaces: Journal of Sedimentary Research78: 579 – 593.

Uresk, J. (1979) Sedimentary environment of the Cretaceous Ferron Sandstone near Caineville, Utah: Brigham Young University Geology Studies, 26: 81-100.

Van den Berg Van Saparoea, A.P.H and Potsma, G (2008) Control of climate change on the yield of river systems in Recent advances in models of siliciclastic shallow-marine stratigraphy: Hampson, G.J., Steel, R.J., Burgess, P.M., and Dalrymple, R.W., *eds*.: Society for Sedimentology Special Publication, 90: 15 - 34.

Van Wagoner, J.C., Mitchum, R.M., Campion, K.M., and Rahmanian, V.D. (1990) Siliciclastic Sequence Stratigraphy in Well Logs, Core, and Outcrops: Concepts for High-Resolution Correlation of Time and Facies: American Association of Petroleum Geologists, Methods in Exploration Series 7: 55 pp.

Whitlock, W.W. (1984) Geology of the Steele Butte Quadrangle, Garfield County, Utah: Brigham Young University Geology Studies, 31: 141 – 165.

Willis, B.J. (1997) Architecture of fluvial-dominated valley-fill deposits in the Cretaceous Fall River Formation: Sedimentology, 44: 735 – 757.

Zaitlin, B.A., Dalrymple, R., and Boyd, R. (1994) The stratigraphic organization of incised-valley systems associated with relative sea-level change *in* Incised-Valley Systems: Origin and Sedimentary Sequences: Dalrymple, R.W., Boyd, R., and Zaitlin, B.A., *eds*.: Society for Sedimentary Geology Special Publication, 51: 45–60.

Zhu, Y., Bhattacharya, J.P., Li, W., Lapen, T.J., Jicha, B.R., and Singer, B.S. (2012) Milankovitch-scale sequence stratigraphy and stepped forced regressions of the Turonian Ferron Notom deltaic complex, south-central Utah, U.S.A.: Journal of Sedimentary Research, 82: 723–746.

APPENDICES

Appendix 1A: Depositional Dip Cross-section

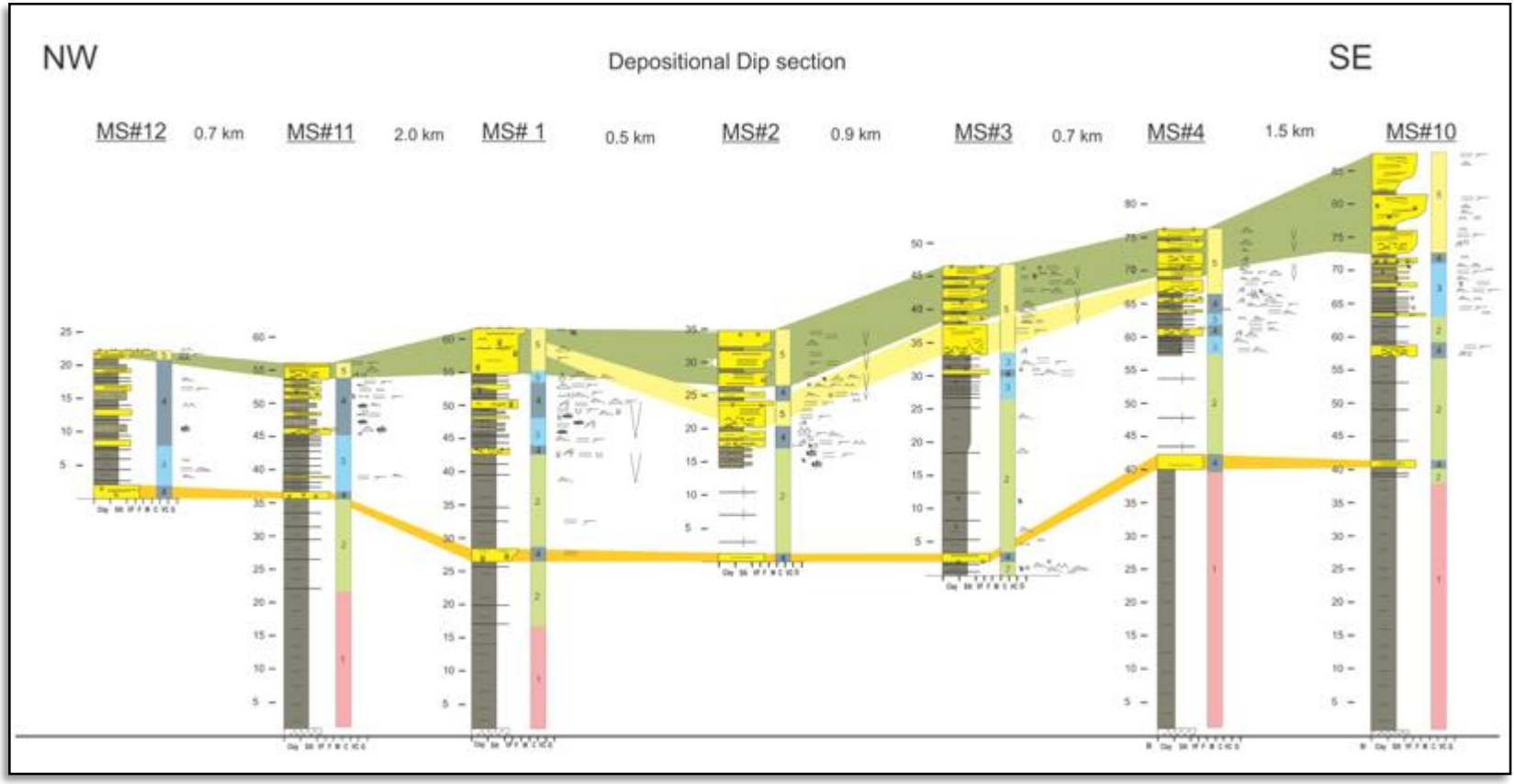

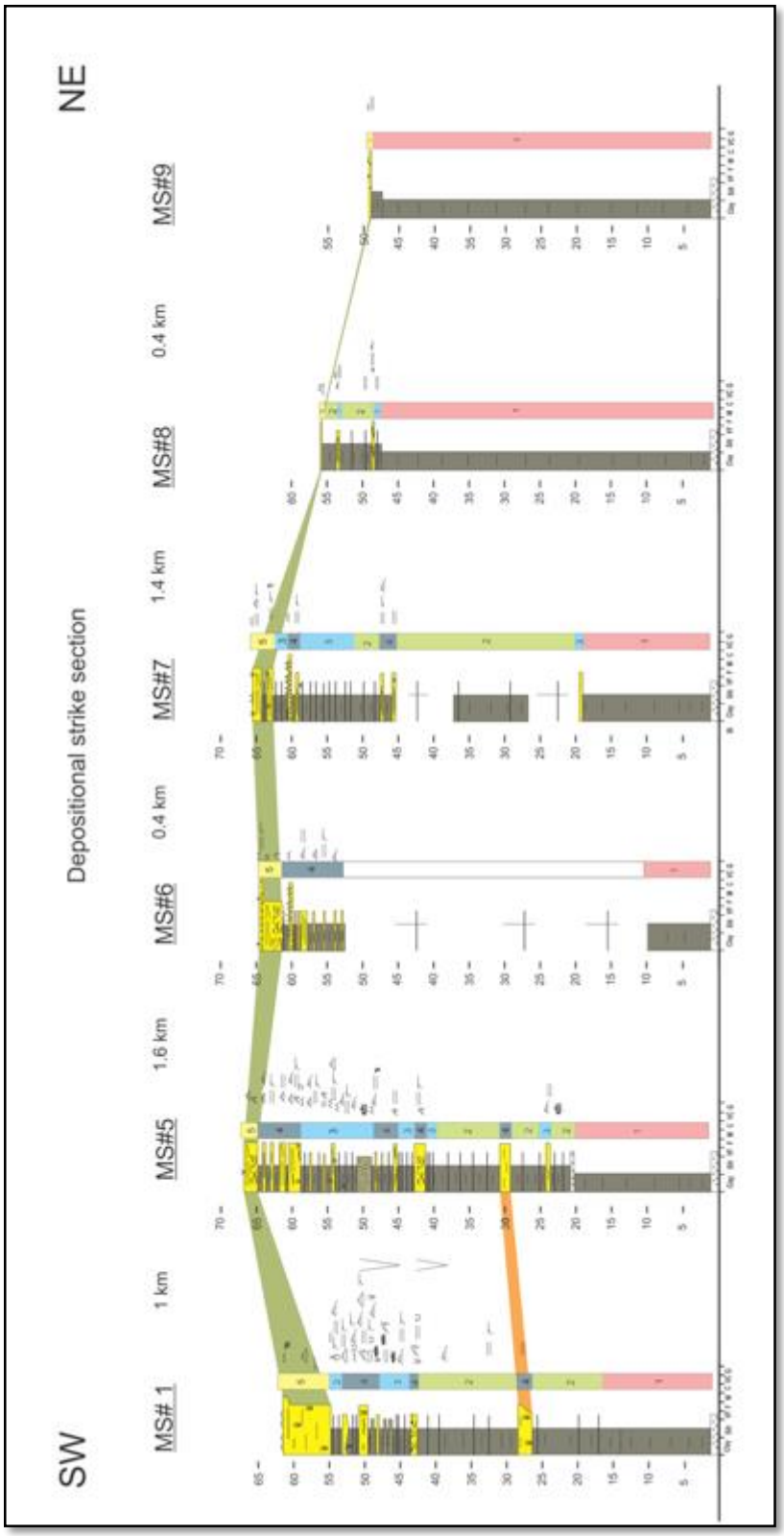

Appendix 1B: Depositional Strike Cross-section

Appendix 2: Measured sections graphic logs

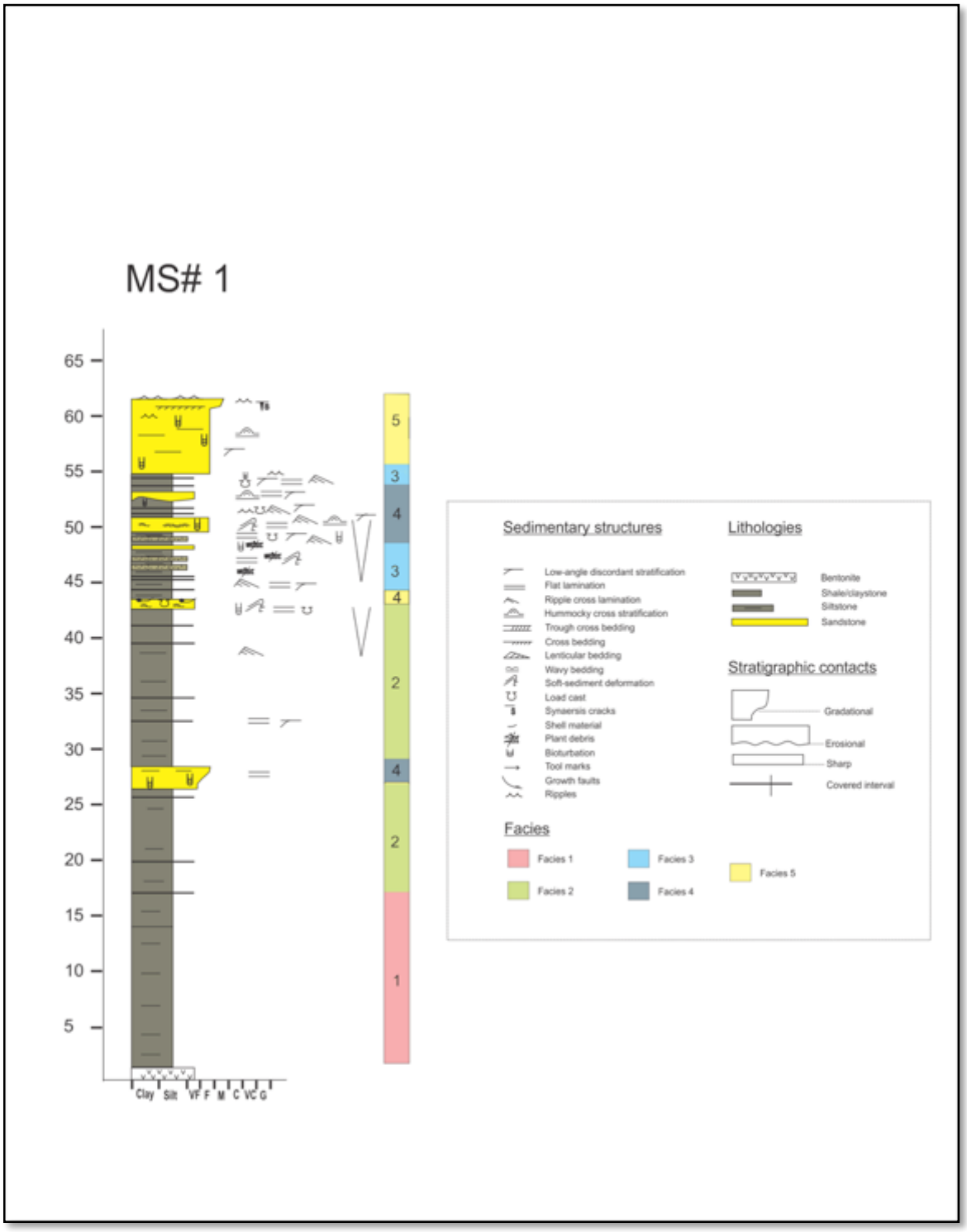

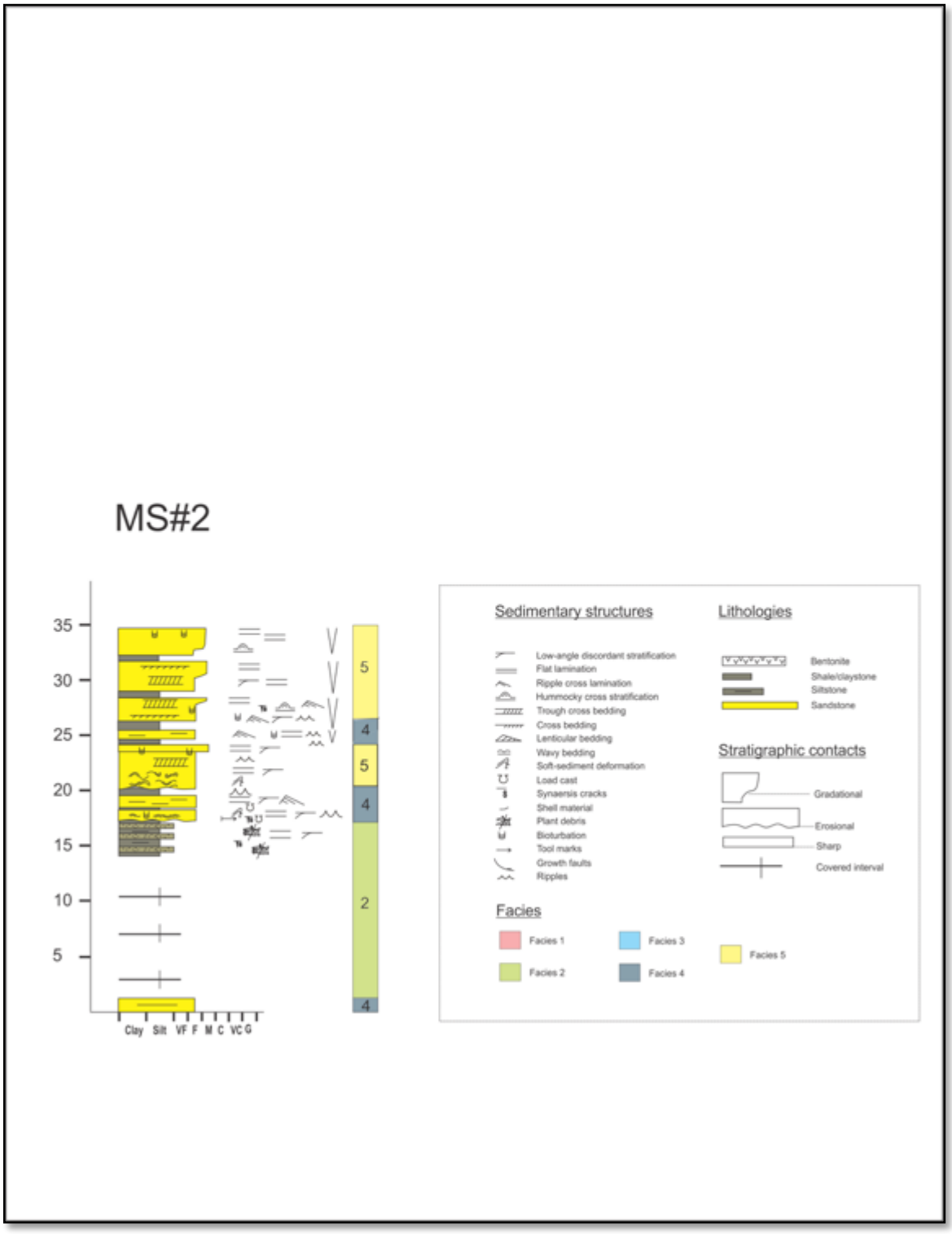
MS#2
35
30
25
20
15
10
5
Clay Silt VF F M C VC G
5
4
5
4
2
4
Sedimentary structures
Low-angle discordant stratification
Flat lamination
Ripple cross lamination
Hummocky cross stratification
Trough cross bedding
Cross bedding
Lenticular bedding
Wavy bedding
Soft-sediment deformation
Load cast
Synaensis cracks
Shell material
Plant debris
Bioturbation
Tool marks
Growth faults
Ripples
Lithologies
Bentonite
Shale/claystone
Siltstone
Sandstone
Stratigraphic contacts
Gradational
Erosional
Sharp
Covered interval
Facies
Facies 1
Facies 2
Facies 3
Facies 4
Facies 5

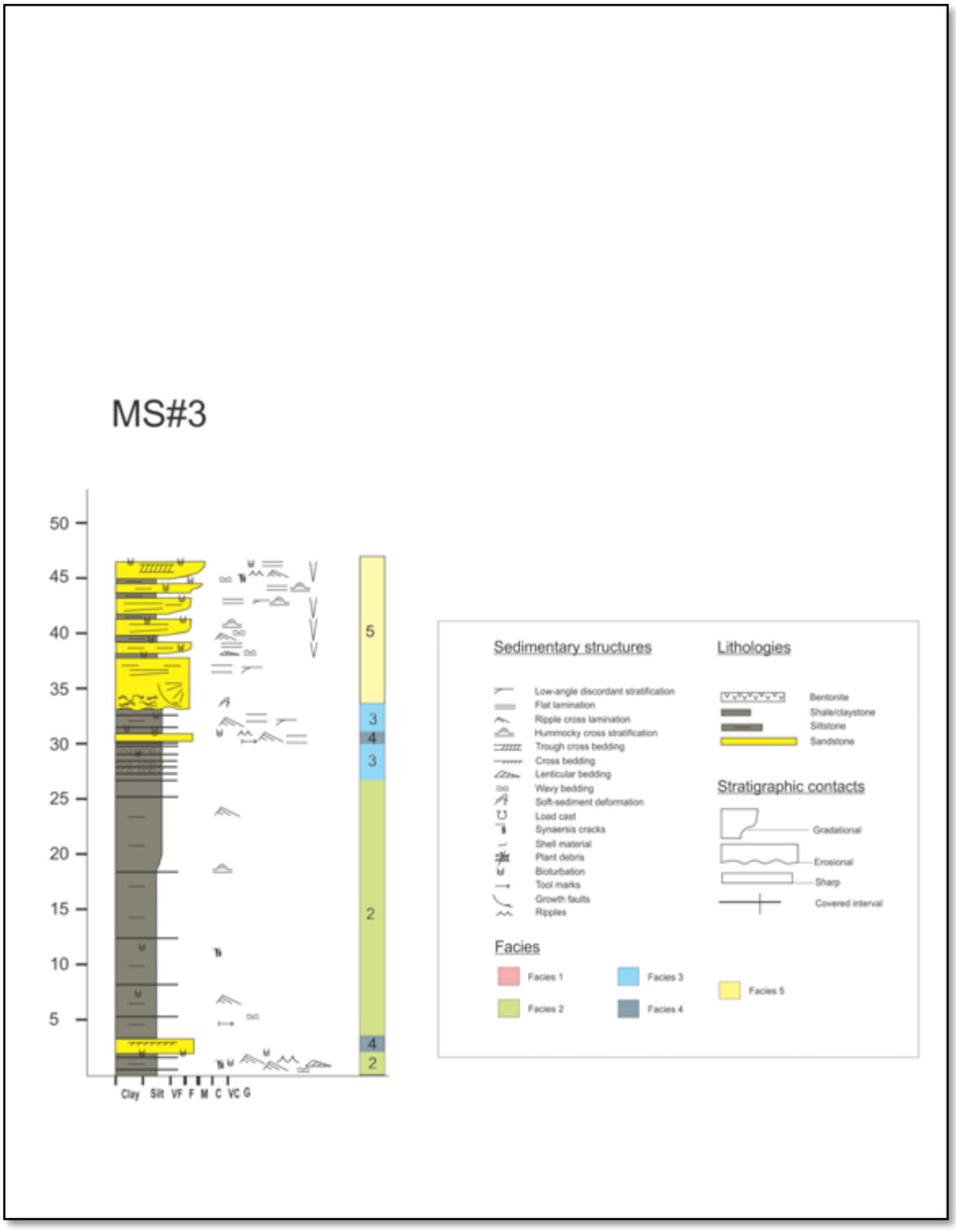
MS#3
50
45
40
35
30
25
20
15
10
5
Clay Silt VF F M C VC G
5
3
4
3
2
4
2
Sedimentary structures
Low-angle discordant stratification
Flat lamination
Ripple cross lamination
Hummocky cross stratification
Trough cross bedding
Cross bedding
Lenticular bedding
Wavy bedding
Soft-sediment deformation
Load cast
Synaersis cracks
Shell material
Plant debris
Bioturbation
Tool marks
Growth faults
Ripples
Lithologies
Bentonite
Shale/claystone
Siltstone
Sandstone
Stratigraphic contacts
Gradational
Erosional
Sharp
Covered interval
Facies
Facies 1
Facies 2
Facies 3
Facies 4
Facies 5

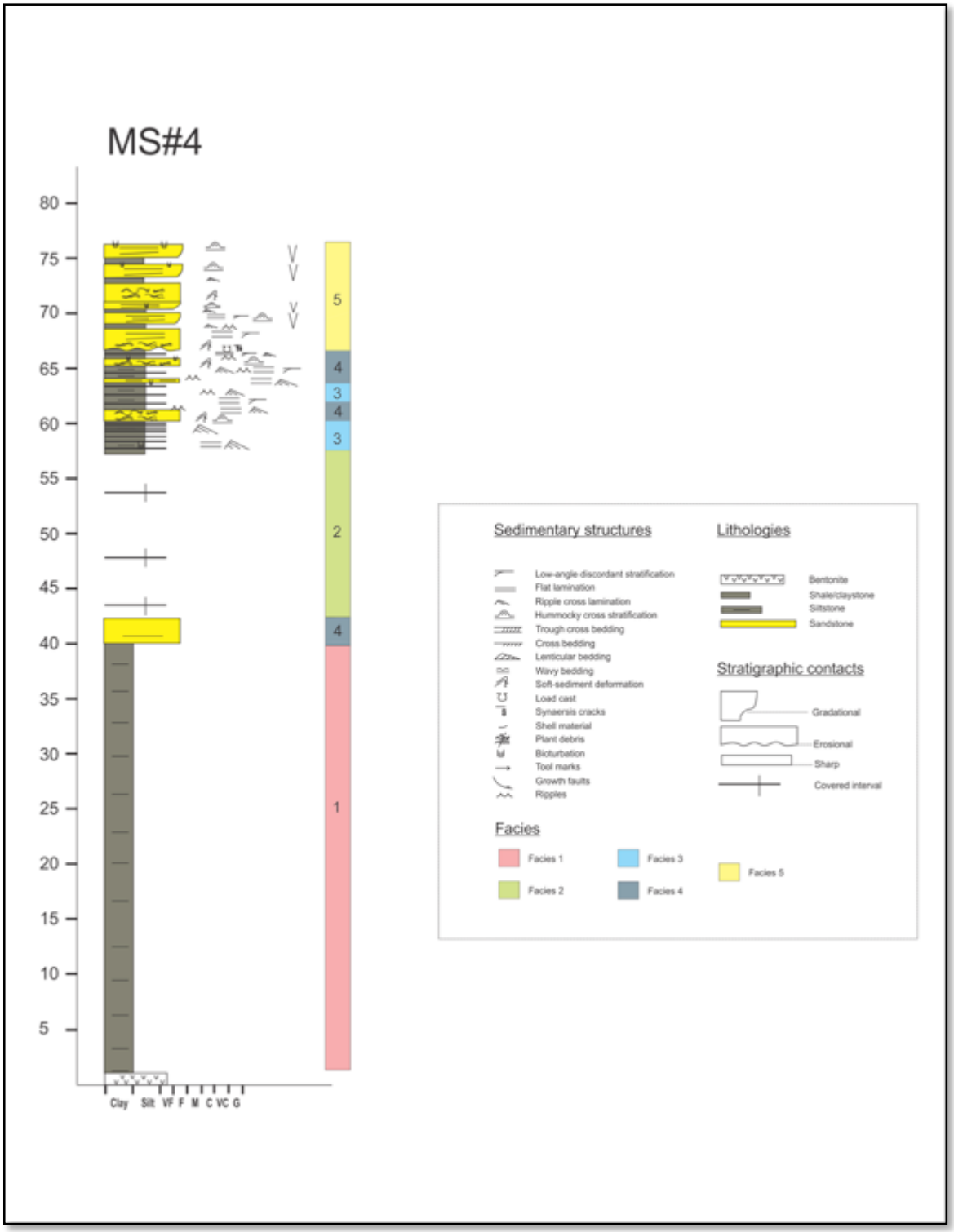
MS#4
80
75
70
65
60
55
50
45
40
35
30
25
20
15
10
5
Clay
Silt
VF
F
M
C
VC
G
5
4
3
4
3
2
4
1
Sedimentary structures
Low-angle discordant stratification
Flat lamination
Ripple cross lamination
Hummocky cross stratification
Trough cross bedding
Cross bedding
Lenticular bedding
Wavy bedding
Soft-sediment deformation
Load cast
Synaersis cracks
Shell material
Plant debris
Bioturbation
Tool marks
Growth faults
Ripples
Lithologies
Bentonite
Shale/claystone
Siltstone
Sandstone
Stratigraphic contacts
Gradational
Erosional
Sharp
Covered interval
Facies
Facies 1
Facies 2
Facies 3
Facies 4
Facies 5

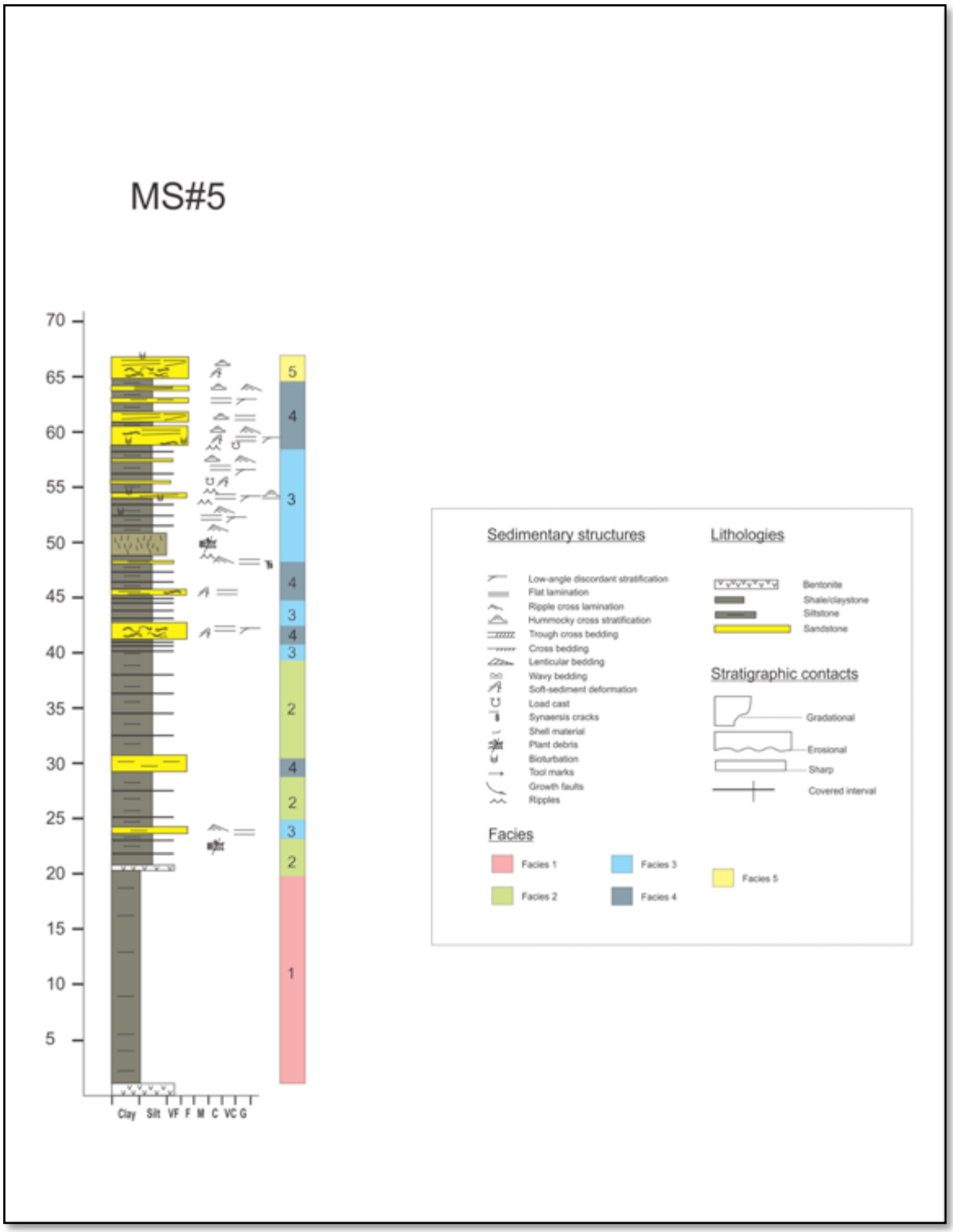
MS#5
70
65
60
55
50
45
40
35
30
25
20
15
10
5
Clay Silt VF F M C VC G
5
4
3
4
3
4
3
2
4
2
3
2
1
Sedimentary structures
Low-angle discordant stratification
Flat lamination
Ripple cross lamination
Hummocky cross stratification
Trough cross bedding
Cross bedding
Lenticular bedding
Wavy bedding
Soft-sediment deformation
Load cast
Synaensis cracks
Shell material
Plant debris
Bioturbation
Tool marks
Growth faults
Ripples
Lithologies
Bentonite
Shale/claystone
Siltstone
Sandstone
Stratigraphic contacts
Gradational
Erosional
Sharp
Covered interval
Facies
Facies 1
Facies 2
Facies 3
Facies 4
Facies 5

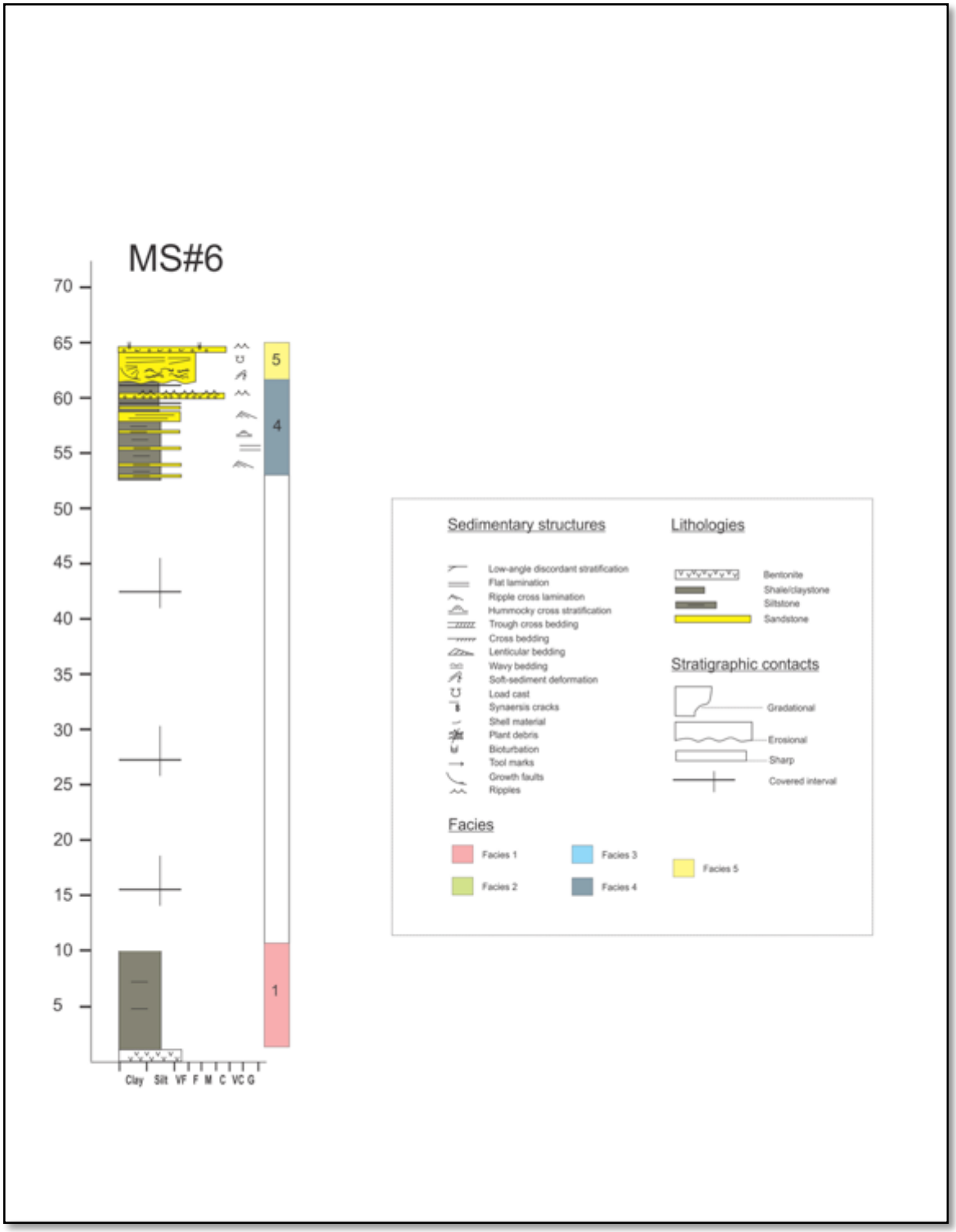
MS#6
70
65
60
55
50
45
40
35
30
25
20
15
10
5
5
4
1
Clay
Silt
VF
F
M
C
VC
G
Sedimentary structures
Low-angle discordant stratification
Flat lamination
Ripple cross lamination
Hummocky cross stratification
Trough cross bedding
Cross bedding
Lenticular bedding
Wavy bedding
Soft-sediment deformation
Load cast
Synaersis cracks
Shell material
Plant debris
Bioturbation
Tool marks
Growth faults
Ripples
Lithologies
Bentonite
Shale/claystone
Siltstone
Sandstone
Stratigraphic contacts
Gradational
Erosional
Sharp
Covered interval
Facies
Facies 1
Facies 2
Facies 3
Facies 4
Facies 5

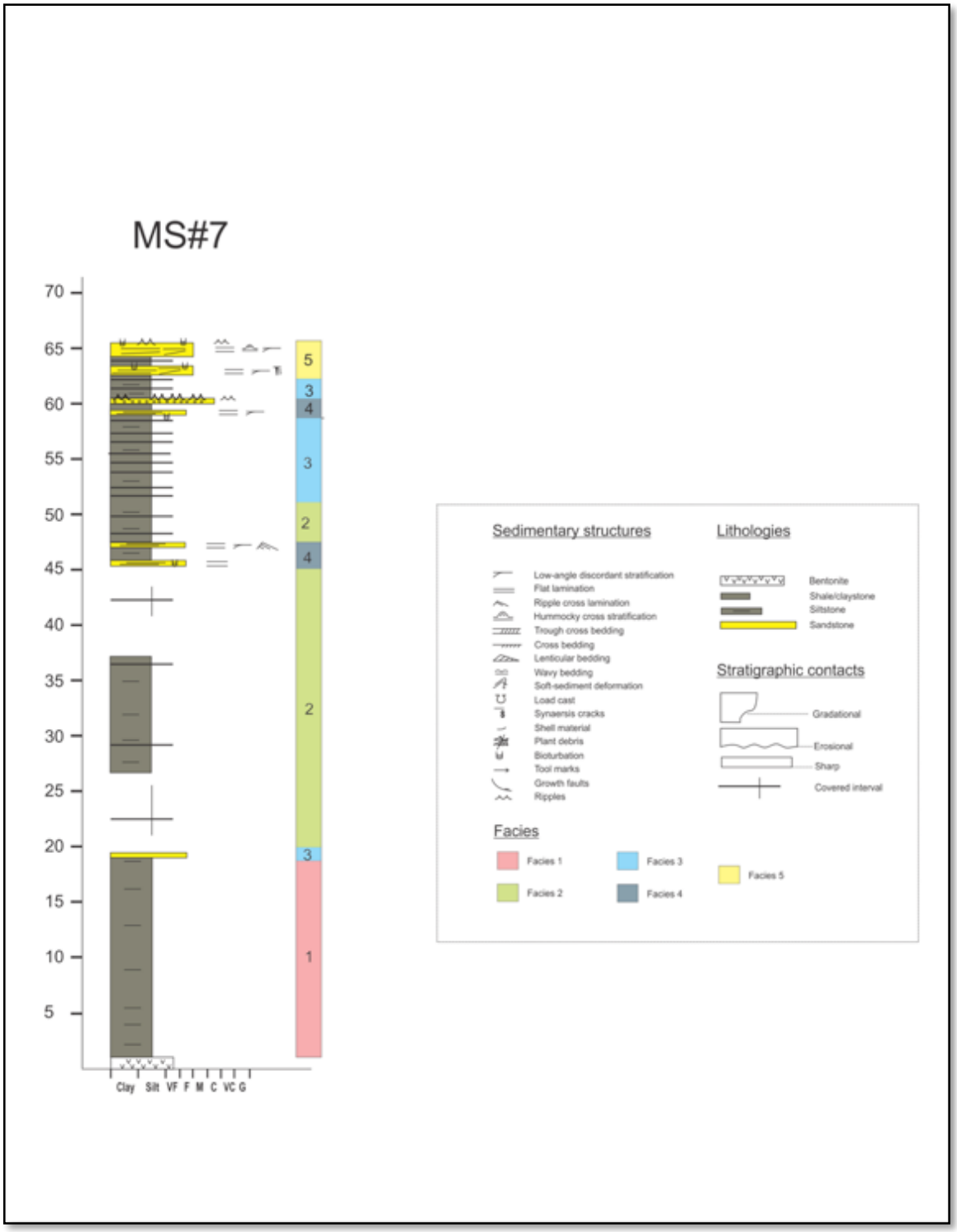
MS#7
70
65
60
55
50
45
40
35
30
25
20
15
10
5
Clay Silt VF F M C VC G
5
3
4
3
2
4
2
3
1
Sedimentary structures
Low-angle discordant stratification
Flat lamination
Ripple cross lamination
Hummocky cross stratification
Trough cross bedding
Cross bedding
Lenticular bedding
Wavy bedding
Soft-sediment deformation
Load cast
Synaersis cracks
Shell material
Plant debris
Bioturbation
Tool marks
Growth faults
Ripples
Lithologies
Bentonite
Shale/claystone
Siltstone
Sandstone
Stratigraphic contacts
Gradational
Erosional
Sharp
Covered interval
Facies
Facies 1
Facies 2
Facies 3
Facies 4
Facies 5

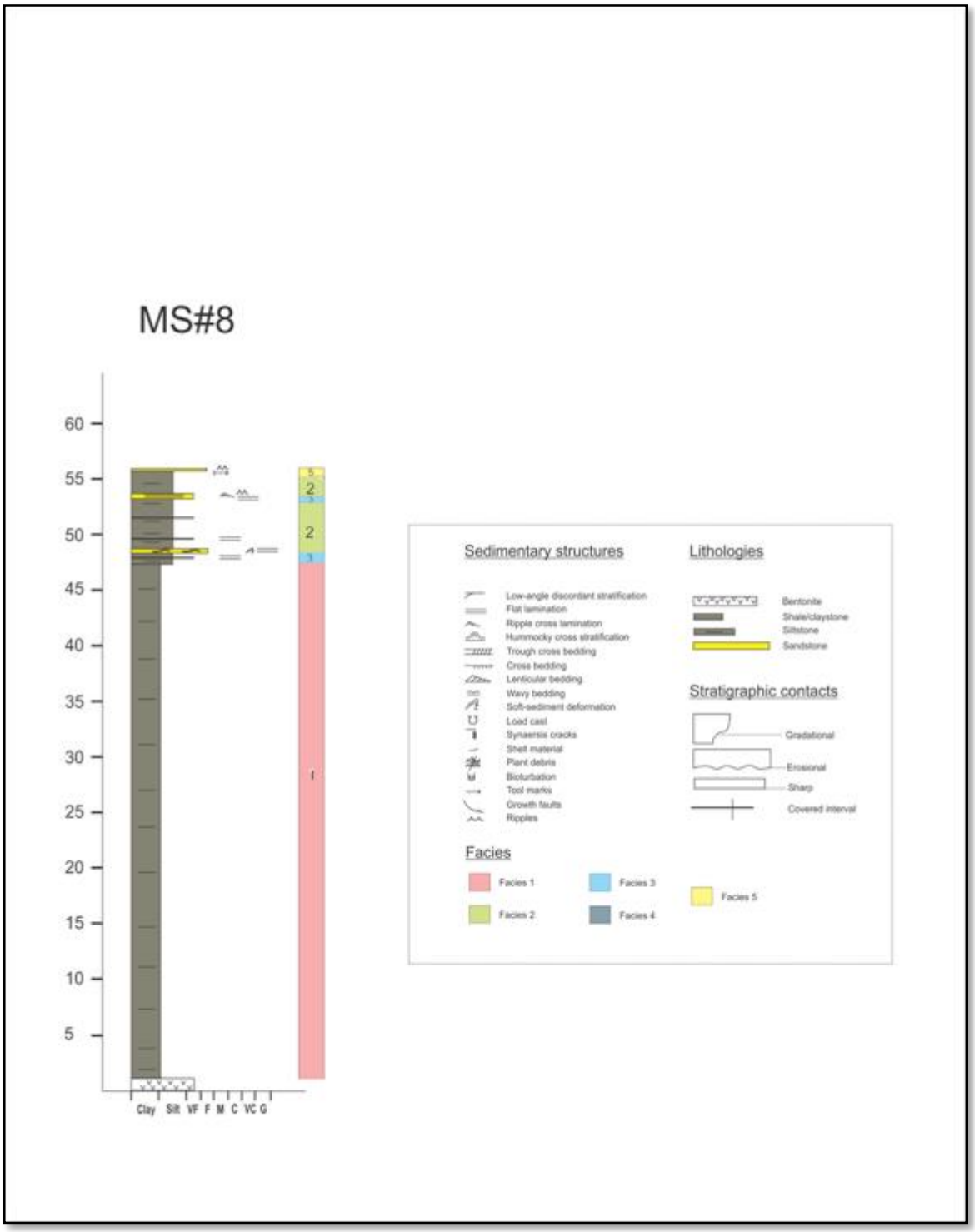
MS#8
60
55
50
45
40
35
30
25
20
15
10
5
Clay
Silt
VF
F
M
C
VC
G
Sedimentary structures
Low-angle discordant stratification
Flat lamination
Ripple cross lamination
Hummocky cross stratification
Trough cross bedding
Cross bedding
Lenticular bedding
Wavy bedding
Soft-sediment deformation
Load cast
Synaersis cracks
Shell material
Plant debris
Bioturbation
Tool marks
Growth faults
Ripples
Lithologies
Bentonite
Shale/claystone
Siltstone
Sandstone
Stratigraphic contacts
Gradational
Erosional
Sharp
Covered interval
Facies
Facies 1
Facies 2
Facies 3
Facies 4
Facies 5

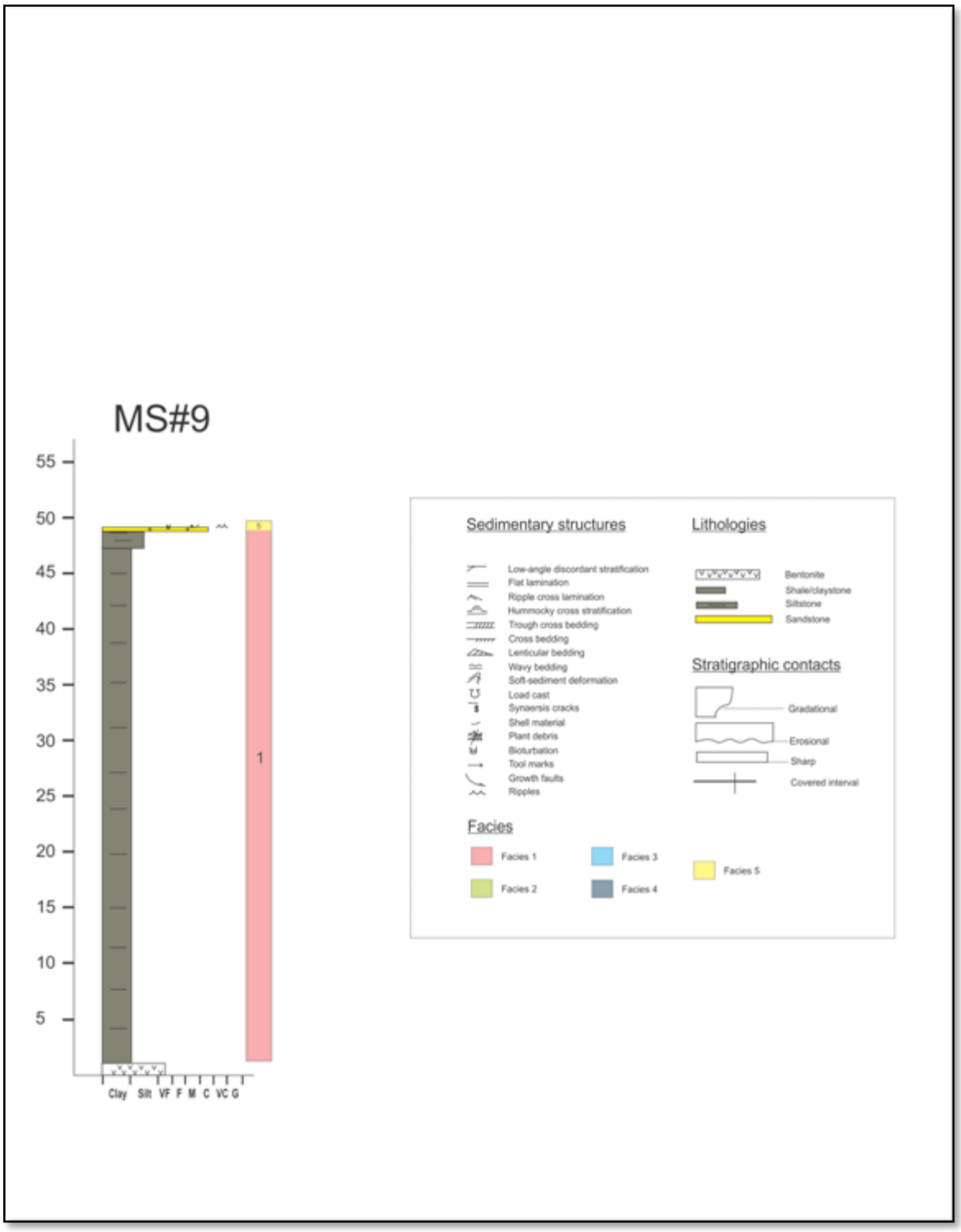
MS#9
55
50
45
40
35
30
25
20
15
10
5
1
Clay
Silt
VF
F
M
C
VC
G
Sedimentary structures
Low-angle discordant stratification
Flat lamination
Ripple cross lamination
Hummocky cross stratification
Trough cross bedding
Cross bedding
Lenticular bedding
Wavy bedding
Soft-sediment deformation
Load cast
Synaensis cracks
Shell material
Plant debris
Bioturbation
Tool marks
Growth faults
Ripples
Lithologies
Bentonite
Shale/claystone
Siltstone
Sandstone
Stratigraphic contacts
Gradational
Erosional
Sharp
Covered interval
Facies
Facies 1
Facies 2
Facies 3
Facies 4
Facies 5

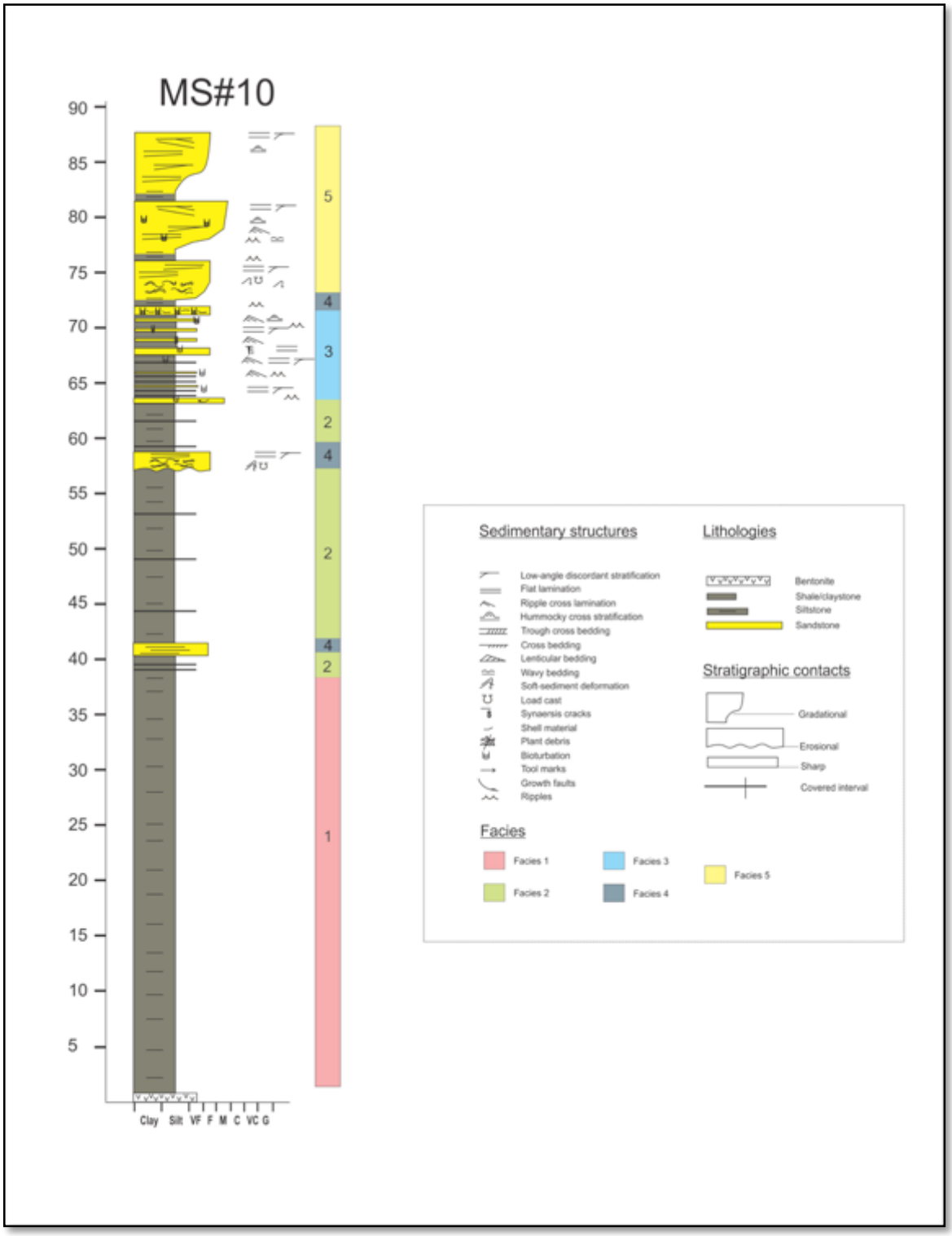
MS#10
90
85
80
75
70
65
60
55
50
45
40
35
30
25
20
15
10
5
Clay Silt VF F M C VC G
5
4
3
2
4
2
4
2
1
Sedimentary structures
Low-angle discordant stratification
Flat lamination
Ripple cross lamination
Hummocky cross stratification
Trough cross bedding
Cross bedding
Lenticular bedding
Wavy bedding
Soft-sediment deformation
Load cast
Synaensis cracks
Shell material
Plant debris
Bioturbation
Tool marks
Growth faults
Ripples
Lithologies
Bentonite
Shale/claystone
Siltstone
Sandstone
Stratigraphic contacts
Gradational
Erosional
Sharp
Covered interval
Facies
Facies 1
Facies 2
Facies 3
Facies 4
Facies 5

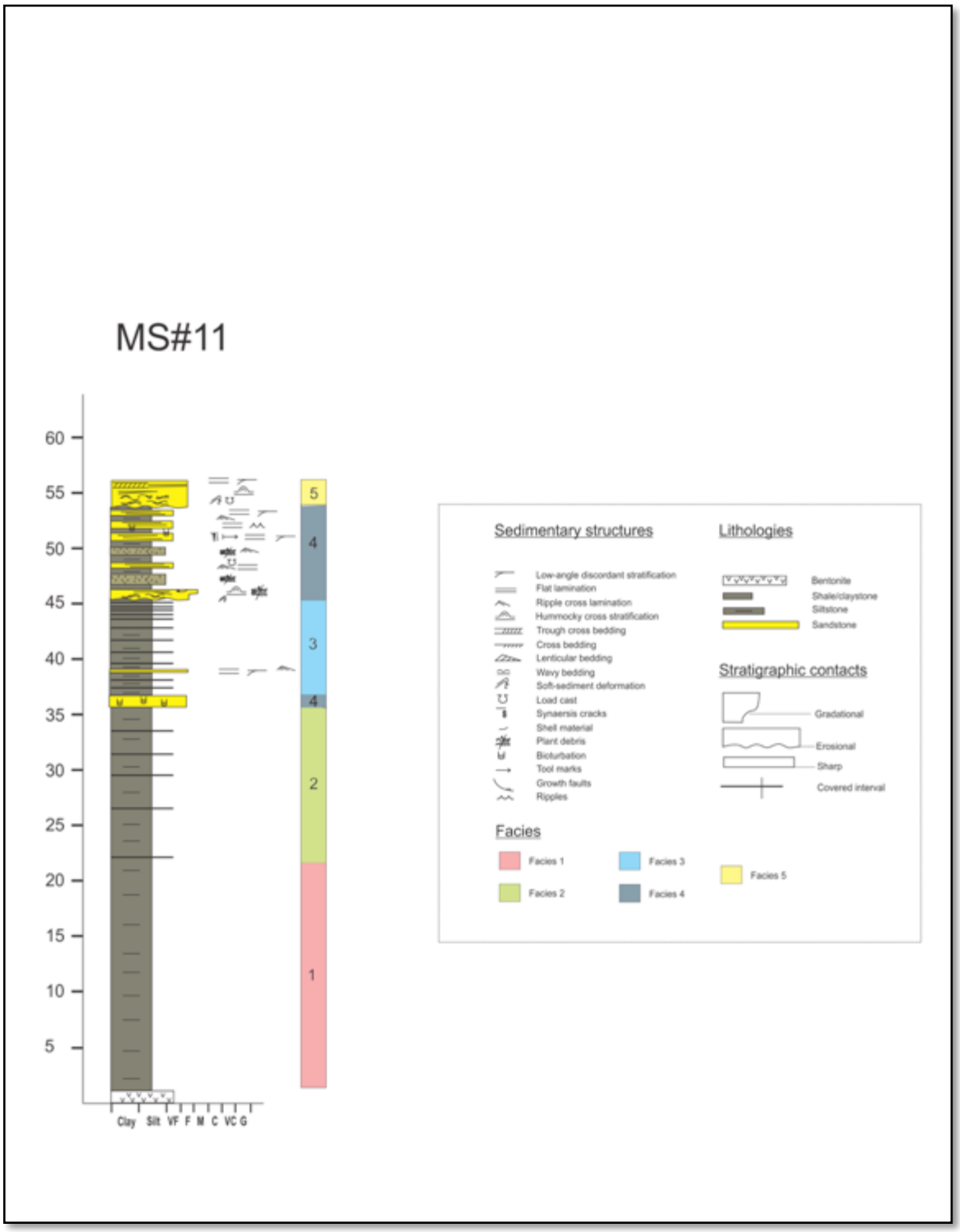
MS#11
60
55
50
45
40
35
30
25
20
15
10
5
Clay Silt VF F M C VC G
5
4
3
4
2
1
Sedimentary structures
Low-angle discordant stratification
Flat lamination
Ripple cross lamination
Hummocky cross stratification
Trough cross bedding
Cross bedding
Lenticular bedding
Wavy bedding
Soft-sediment deformation
Load cast
Synaersis cracks
Shell material
Plant debris
Bioturbation
Tool marks
Growth faults
Ripples
Lithologies
Bentonite
Shale/claystone
Siltstone
Sandstone
Stratigraphic contacts
Gradational
Erosional
Sharp
Covered interval
Facies
Facies 1
Facies 2
Facies 3
Facies 4
Facies 5

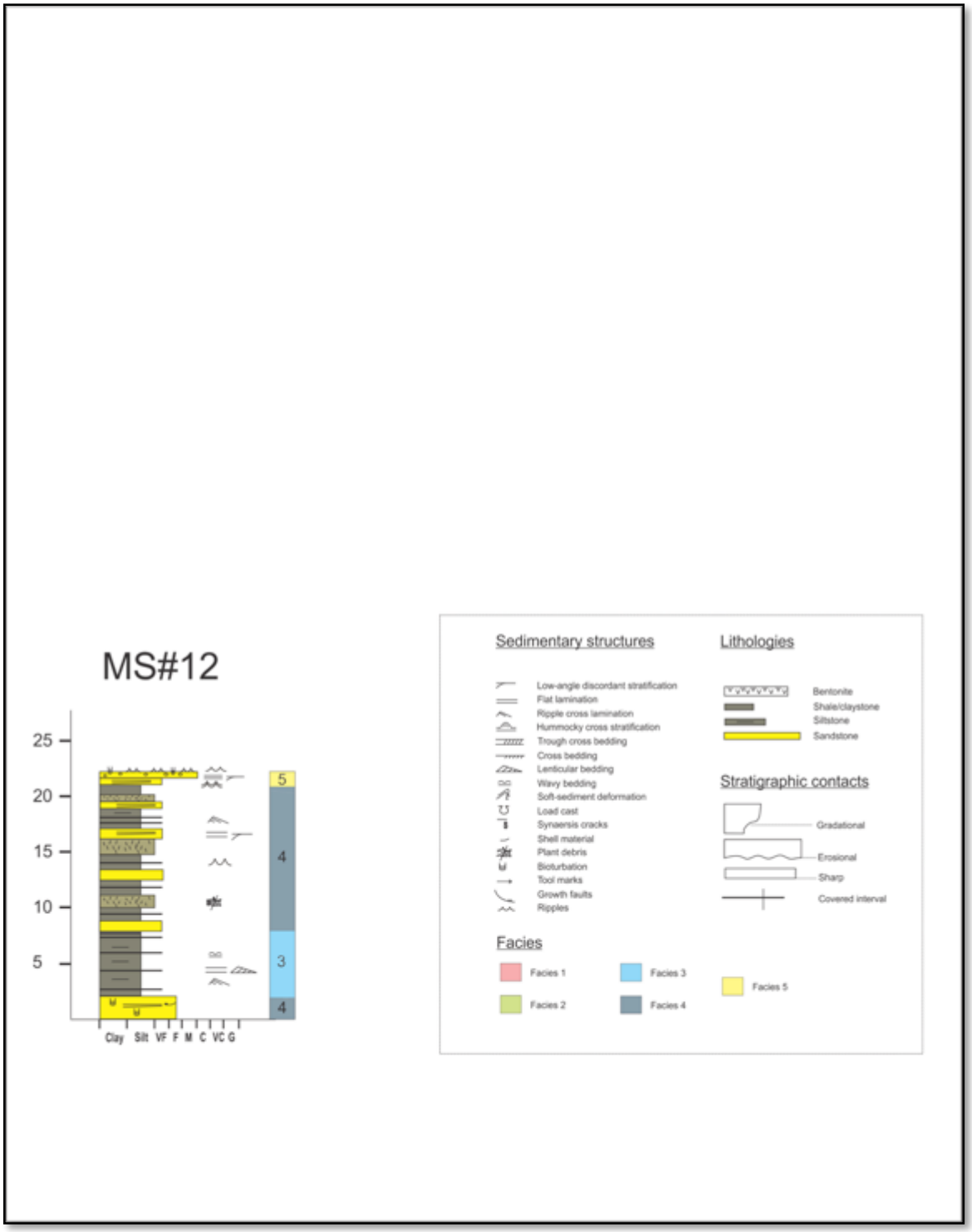
MS#12
25
20
15
10
5
Clay Silt VF F M C VC G
5
4
3
4
Sedimentary structures
Low-angle discordant stratification
Flat lamination
Ripple cross lamination
Hummocky cross stratification
Trough cross bedding
Cross bedding
Lenticular bedding
Wavy bedding
Soft-sediment deformation
Load cast
Synaensis cracks
Shell material
Plant debris
Bioturbation
Tool marks
Growth faults
Ripples
Lithologies
Bentonite
Shale/claystone
Siltstone
Sandstone
Stratigraphic contacts
Gradational
Erosional
Sharp
Covered interval
Facies
Facies 1
Facies 2
Facies 3
Facies 4
Facies 5

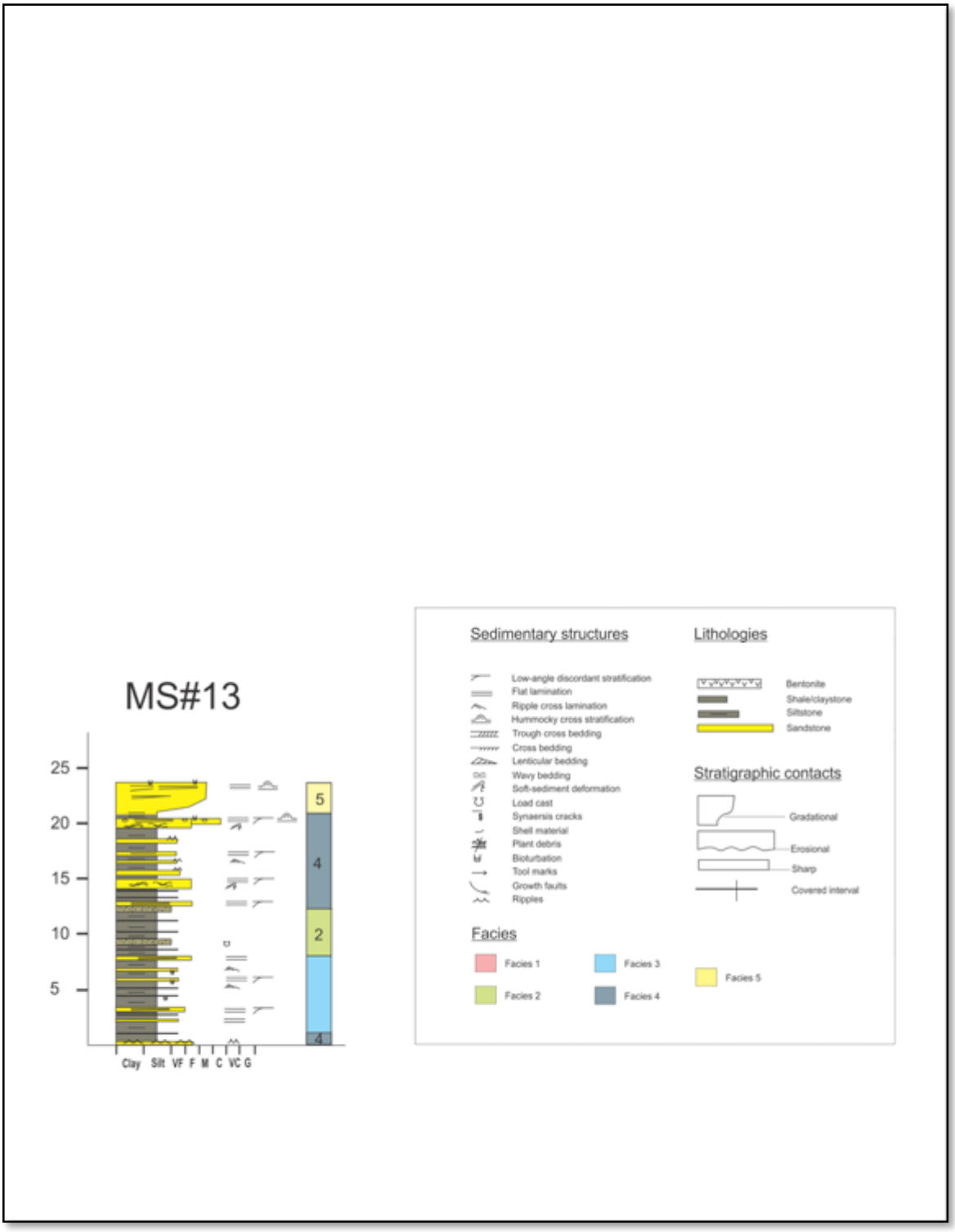
MS#13
25
20
15
10
5
Clay
Silt
VF
F
M
C
VC
G
5
4
2
4
Sedimentary structures
Low-angle discordant stratification
Flat lamination
Ripple cross lamination
Hummocky cross stratification
Trough cross bedding
Cross bedding
Lenticular bedding
Wavy bedding
Soft-sediment deformation
Load cast
Synaersis cracks
Shell material
Plant debris
Bioturbation
Tool marks
Growth faults
Ripples
Lithologies
Bentonite
Shale/claystone
Siltstone
Sandstone
Stratigraphic contacts
Gradational
Erosional
Sharp
Covered interval
Facies
Facies 1
Facies 2
Facies 3
Facies 4
Facies 5

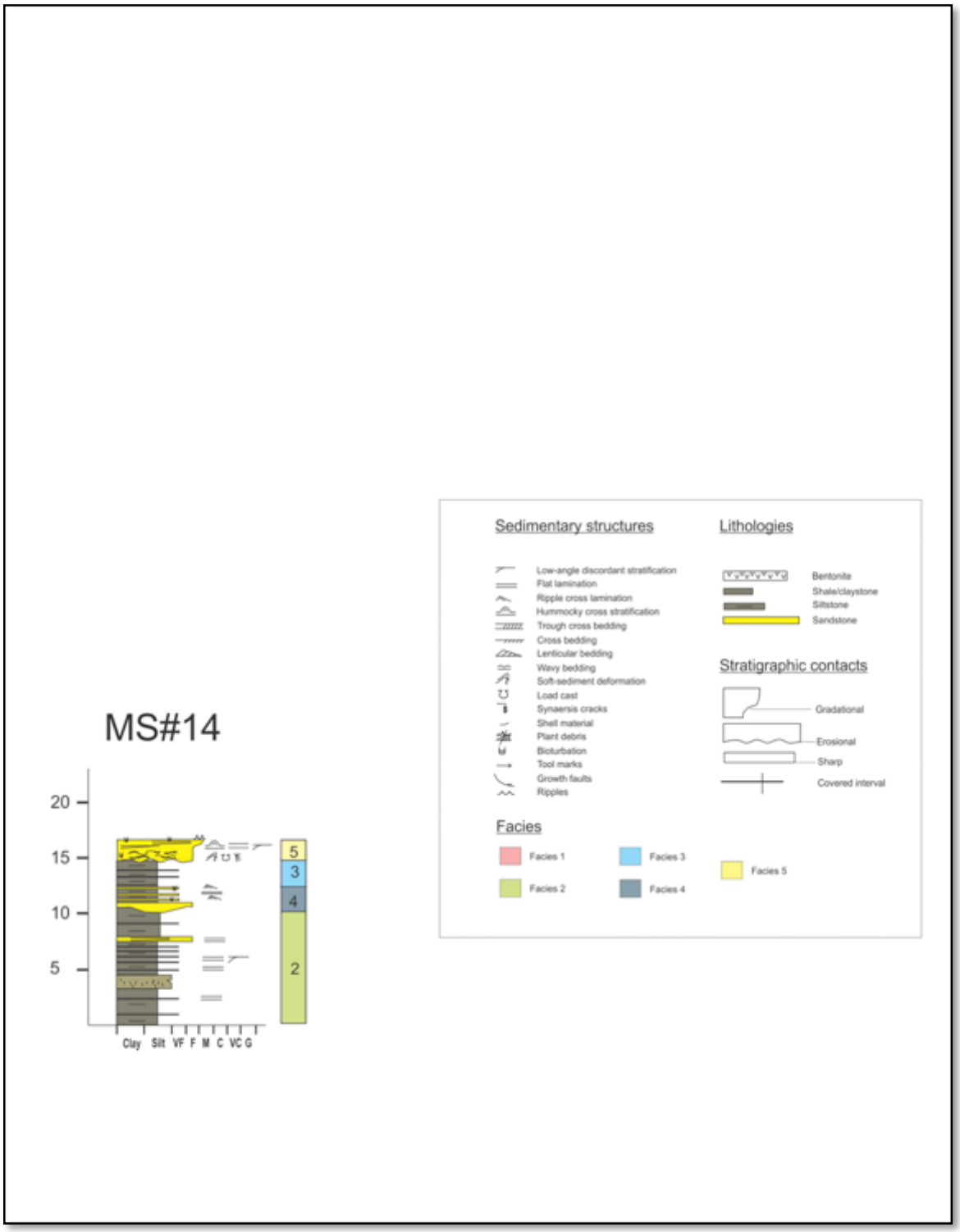
MS#14
20
15
10
5
Clay
Silt
VF
F
M
C
VC
G
5
3
4
2
Sedimentary structures
Low-angle discordant stratification
Flat lamination
Ripple cross lamination
Hummocky cross stratification
Trough cross bedding
Cross bedding
Lenticular bedding
Wavy bedding
Soft-sediment deformation
Load cast
Synaersis cracks
Shell material
Plant debris
Bioturbation
Tool marks
Growth faults
Ripples
Lithologies
Bentonite
Shale/claystone
Siltstone
Sandstone
Stratigraphic contacts
Gradational
Erosional
Sharp
Covered interval
Facies
Facies 1
Facies 2
Facies 3
Facies 4
Facies 5

Appendix 3: Facies Table

Facies	Lithology	Physical Structures	Biogenic Structures	Interpretation
1	Thinly laminated, locally fissile, claystone and fine-grained mudstone, with thin local bentonite beds. Siltstone ratio increases up-section	Fissile, parallel lamination	Largely unbioturbated BI=0	Offshore
2	Thinly laminated dark grey siltstone with very fine- to fine-grained sandstone.	Sandstones show parallel lamination, ripple cross-lamination, small HCS	Bioturbation is low and sporadic, BI= 0-3: *Planolites*, *Protovirgularia*, *Lockeia*, and small *Diplocraterion. Diminutive size,* low diversity, with a maximum of three different ichnogenera	Prodelta
3	Thinly interbedded dark grey siltstone with very fine- to fine-grained sandstone (< 0.2 m)	Stratified sandstone: hummocky cross-stratification (HCS), Ripple cross-lamination, and flat to low-angle cross bedding. Some sandstone beds tops have wave ripples. Sandstone bodies thicken and become abundant up-section	Siltstones are unbioturbated; bioturbation in sandstone is low, BI= 0-2: *Planolites*, *Diplocraterion*, *Lockeia*, and *Cylindrichnus. Diminutive size,* low diversity, with no more than two ichnogenera	Distal Delta Front

4	Thickly interbedded siltstone (fine- and coarse-grained) and very fine- to fine-grained sandstone. Sandstone beds have sharp contacts with underlying siltstones	Sandstone bodies show HCS, ripple cross-lamination, flat-to-low angle cross-bedding, convolute bedding, soft sediment deformation (SSD), wave ripples (on top of sandstone beds), and loading	Sandstones show low to moderate bioturbation intensity, BI= 1-3: *Planolites, Lockeia, Teichichnus, Thalassinoides, Diplocraterion, Gyrochorte, Rhizocorallium, and Taenidium.* Diminutive size, mostly low diversity, some beds show higher diversity with up to four different ichnogenera.	Medial Delta Front
5	Amalgamated, massive, sharp-based fine- to medium-grained sandstone. Three variants recognized: 1. soft-sediment deformed, 2. stratified, 3. rotated masses.	Observed sedimentary structures include large-scale hummocky cross-stratification (HCS), flat to low-angle cross-lamination, ripple cross-lamination, convolute bedding, loading, and trough cross bedding.	Bioturbation is variable, but shows generally low to moderate intensities (BI= 0-2; 2-4): *Planolites, Diplocraterion, Teichichnus, Thalassinoides, Cylindrichnus, Lockeia, Ophiomorpha, Taenidium, and* navichnia. Mostly small in size, low diversity, some beds show higher diversity with up to four different ichnogenera.	Proximal Delta Front

Appendix 4: Paleocurrent data

MS#1	MS#2	MS#3	MS#4	MS#5	MS#8	MS#10	MS#11	MS#12
92	79	21	125	26	120	35	123	44
93	98	21	196	28	118	40	137	55
97	103	28		30	167	57	139	83
99	108	53		32		62		105
105	115	62						120
129	119	68						
130	122	68						
132	127	70						
133	132	74						
134	145	76						
134	146	102						
137	146	107						
158	160	109						
162	178	134						
172	179	152						
	186	159						
	198	226						
	232	248						
	263	258						
		292						